THE BIHARMONIC BOUNDARY VALUE PROBLEM AS APPLIED TO A MEMBRANE HAVING IRREGULAR SHAPE

By

HOWARD WESLEY SMITH

Bachelor of Science
Wichita State University
Wichita, Kansas
1951

Master of Science
Wichita State University
Wichita, Kansas
1958

Submitted to the faculty of the Graduate College
of the Oklahoma State University
in partial fulfillment of the requirements
for the degree of
DOCTOR OF PHILOSOPHY
May 1968

THE BIHARMONIC BOUNDARY VALUE PROBLEM

AS APPLIED TO A MEMBRANE

HAVING IRREGULAR SHAPE

Thesis Approved:

R. E. Chapel
Thesis Adviser

Ladislaus J Fila

R L Lowery

Thomas Scott Dean

N Durham
Dean of the Graduate College

PREFACE

The research work described in this document was sponsored by the Air Force Office of Scientific Research, Office of Aerospace Research, United States Air Force, and The Boeing Company, Wichita Division. The primary agreement was grant No. AF-AFOSR-1153-66 to Oklahoma State University. The secondary agreement was Oklahoma State University purchase order No. 68732 to The Boeing Company.

The motivation for the research work is deeply rooted in my desire to bring more powerful analytical and experimental tools to the practicing structural designers and stress analysts who are heavily burdened with the responsibility of insuring structural safety. They will freely admit that their methods are not totally satisfactory, and they hope that the fruits of research on higher planes will be of value to them.

I wish to acknowledge the cooperation of my wife, Esther, and my sons for their prior approval, the inconveniences I have caused them, and the material aid they donated. I am indebted especially to Professor Raymond E. Chapel, my thesis adviser, and Professors R. L. Lowery, L. J. Fila, and T. S. Dean. Many other faculty and staff advised me in a variety of matters: R. MacVicar, J. H. Boggs, D. R. Haworth.

The Boeing Company awarded me a Doctoral Leave Scholarship which made the residency possible. I am especially indebted to L. L. Gore, D. E. Strand, B. W. Hodges, J. J. Clark, and L. W. Whiteside of the Wichita Division for their encouragement and confidence in me.

TABLE OF CONTENTS

LIST OF TABLES

LIST OF FIGURES

NOMENCLATURE

Symbol	Description	Unit
Latin:		
a, b, c, ...	dimensions	inches
k, l, m, n	integers	-
t	thickness	inches
u, v, w	displacements in x, y, z	inches
x, y, z	spatial coordinates	-
A, B, C, ...	constants	-
E	Young's modulus	lbs/sq.in.
Greek:		
α	selvedge point ratio	-
γ	shear strain	in./in.
δ	mesh spacing	inches
δ_1	short "string" distance	inches
ε	axial strain	in./in.
σ	axial stress	lbs/sq.in.
ν	Poisson's ratio	in./in.
τ	shear stress	lbs/sq.in.
Φ	Airy stress function	-

Symbol	Description	Unit
Special Symbols:		
∂	partial derivative operator	-
∇^2	Laplacian operator	-
$\equiv$	mathematical definition	-

CHAPTER I

INTRODUCTION

The plane problem of the theory of elasticity occurs in the design of space vehicles, airplanes, land vehicles, ships, and submarines. Teodorescu's survey paper [1][1] is evidence of the importance of the subject and contains 225 references to previous work in the field. Teodorescu cites the history, derivation, and computational methods for the plane problem.

Practicing engineers are confronted with calculating the stresses in plane membranes having boundary curvature and complex distributions of edge tractions and shear flows. The solution for the biharmonic equation for such problems is not available to the average engineer. This project was undertaken to provide an analysis method to solve plane stress problems and to provide experimental data for comparison.

Plane stresses are inherently involved with vehicle safety and must be precisely determined for structures. Because the plane stress problem occurs frequently in practice, solution to the elastostatic boundary value problem is formulated for a singly-connected region having a piecewise-smooth contour. Arbitrary pairs of normal and tangential stresses are specified at every point on the boundary.

---

[1] Numbers in small brackets refer to references in the bibliography.

The biharmonic equation is written in terms of its central finite difference equivalent on a square mesh drawn to cover the region of interest and to extend sufficiently to include fictitious points. Boundary stresses are assumed to be quadratic polynomials over each mesh interval. The coefficients of the linear terms and the constant are selected to allow the Airy function and slopes to be continuous at the boundary nodes. A linear algebraic equation is written for each node. The set of equations is written in matrix notation and solved directly on a digital computer. Stresses are obtained from the known values of the Airy stress function by calculating second partial derivatives.

An experimental specimen was designed, manufactured, and instrumented to provide measured data. A semi-monocoque cylindrical shell containing a full web stiffened bulkhead (Figure 1) provided the necessary test region and the desired boundary stress complexity.

Strain data for regions having boundary curvature and stress complexity is virtually non-existent in the available literature. Although the experiment was specifically designed for this research, provision was made for future analysis and experimentation. Bonded epoxy-backed strain gages were used for primary measurement.

Chapter II contains a description of the analytical method. Chapter III contains a description of the specimen, loading fixture, instrumentation, and the experimental data obtained. Chapter III also has a comparison of the analytical and experimental results. Chapter IV contains a summary of the work done, conclusions, and suggestions for possible future efforts.

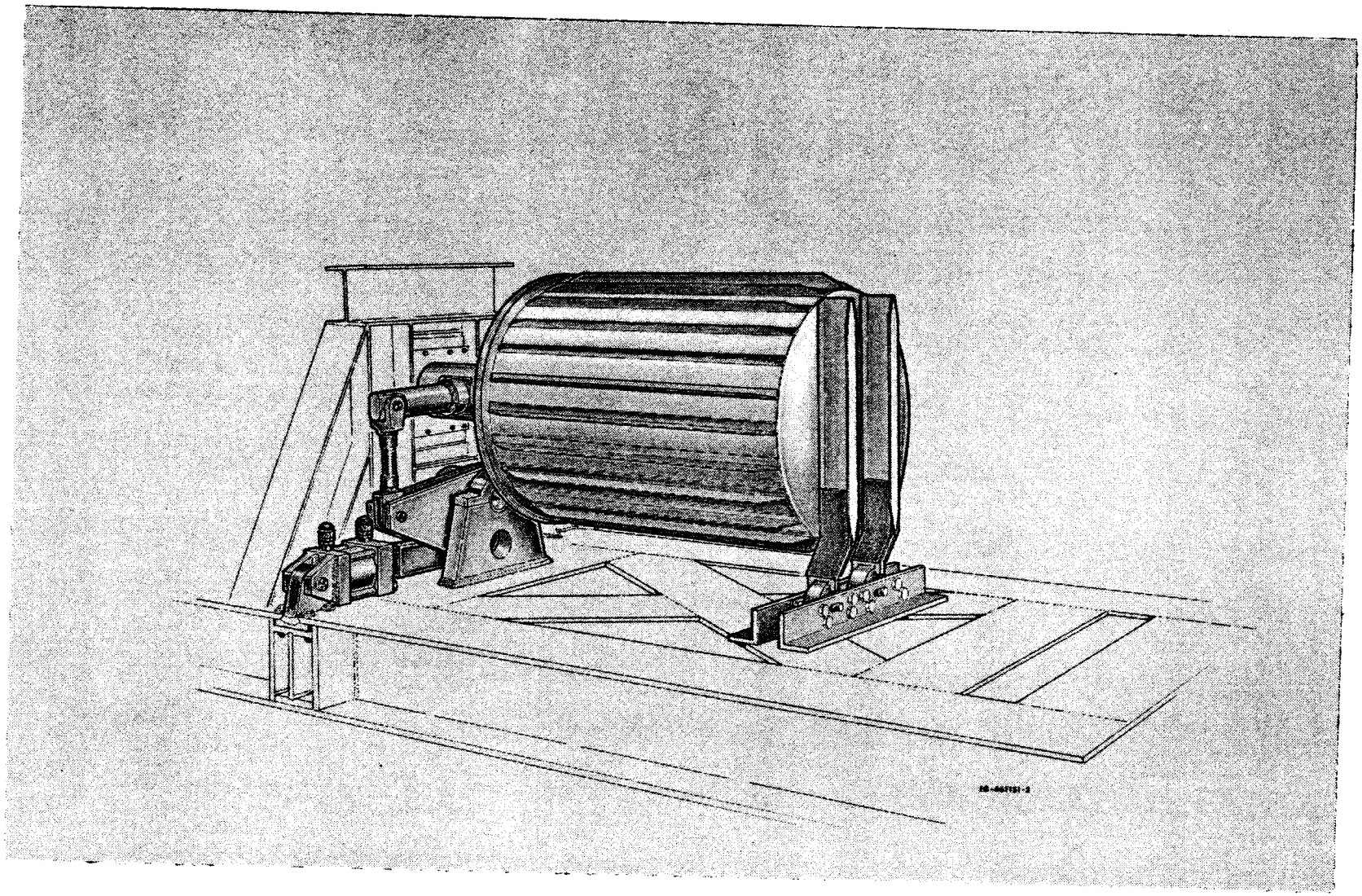

Figure 1. Experimental Specimen Installation

CHAPTER II

ANALYSIS METHOD

The analysis method developed here is a composite of the classical finite difference method described by Timoshenko and Goodier [2] and the relaxation method used by Allen [3]. Inclusion of the newly developed biharmonic boundary value integration link and the Airy Stress Function link renders the analysis method "direct". The word "direct" is defined here to mean "step-by-step", in the same sense that a beam analysis is direct. The method is analogous to beam stress analysis: region to be analyzed is first drawn to scale (beam is drawn); equilibrium is analyzed (beam reactions are calculated); Airy function values are found (moment diagram is drawn); and stresses are obtained from the Airy function (flexural stresses are obtained from the bending moment).

Details of each step in the analysis method are given below, and each step is illustrated with a sample numerical calculation. The shape chosen for analysis is identical to that selected for experimental investigation and is described in succeeding chapters.

The first fundamental problem of the theory of elasticity is characterized by the biharmonic equation,

$$\nabla^4 \Phi = 0 \tag{1}$$

Mathematical derivation of the biharmonic equation is given in reference [2]. It is the counterpart of the Dirichlet problem for

Laplace's equation and will be referred to as the "Airy Problem" in honor of his pioneering work [4]. Accordingly, the biharmonic boundary stress value integration will be called "Airy Integration". The matrix of coefficients formed by the simultaneous equations will be called the "Airy Matrix". The stress function may be geometrically interpreted as a surface with the z-coordinate as phi. It is understood that mid-plane of the stressed membrane lies in the x-y plane.

Graphical Preliminaries

The first step in the proposed analysis method is a scale drawing of the boundary curve for the region to be investigated, as illustrated in Figure 2. The physical location of the analyzed region is described in the experimental portion of this report. The coarse grid layout was drawn, and the nodal points were numbered and coded, resulting in nine regular nodes, fifteen boundary nodes, and thirteen fictitious nodes.

Two mesh lengths were analytically investigated in this research. A fine grid, having a half-inch grid length, resulted in 48 regular nodes, 30 boundary nodes and 28 fictitious nodes. The fine grid diagram is illustrated in Figure 3.

Equilibrium Analysis

Tractions and shears were presumed to be known everywhere on the boundary for formulation of the first fundamental problem. The boundary forces were derived from the rosette data and are presented graphically in Figure 4. Stresses for the boundary value integration were read from Figure 4 at points halfway between the boundary nodes, and are

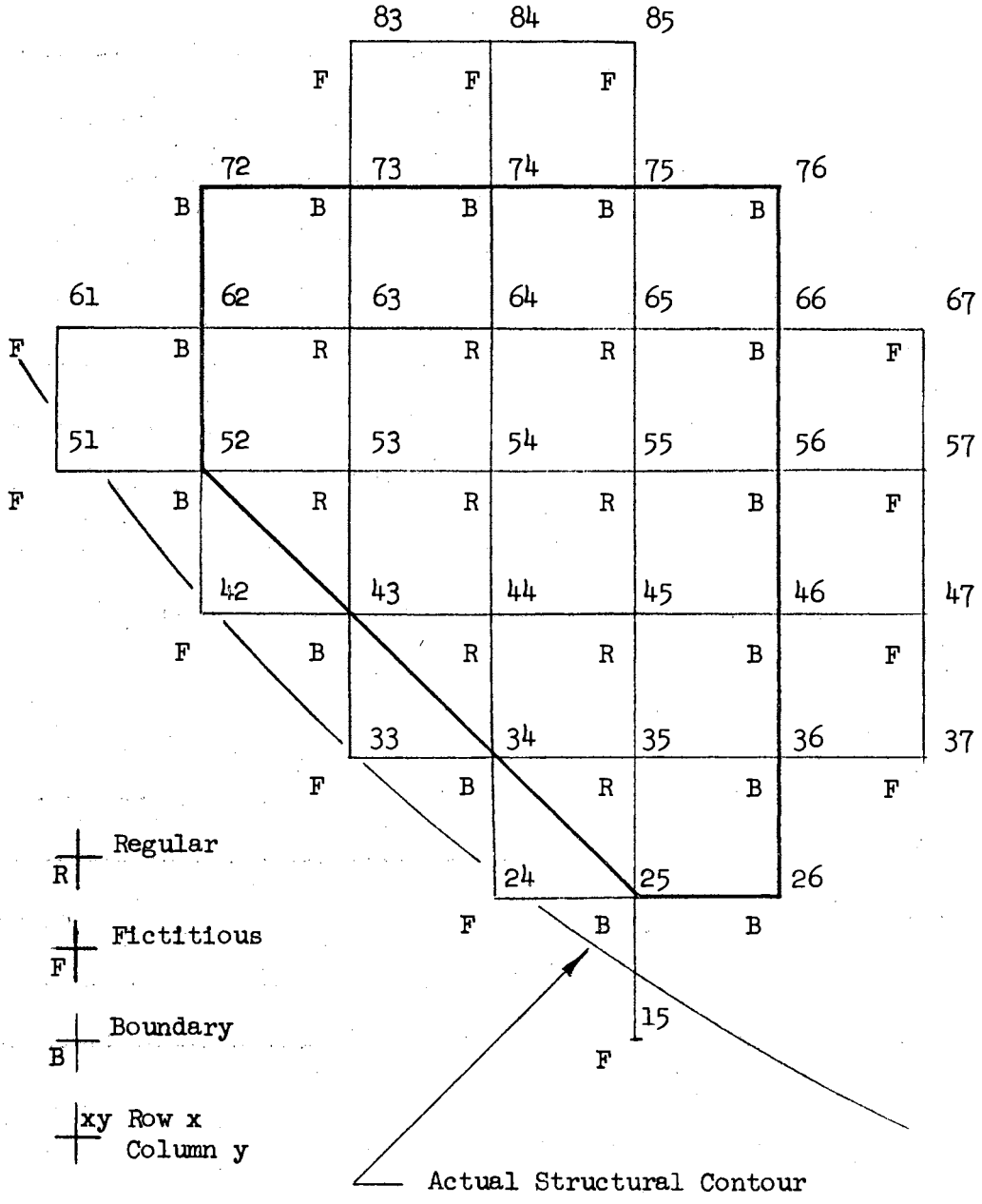

Figure 2. Coarse Grid

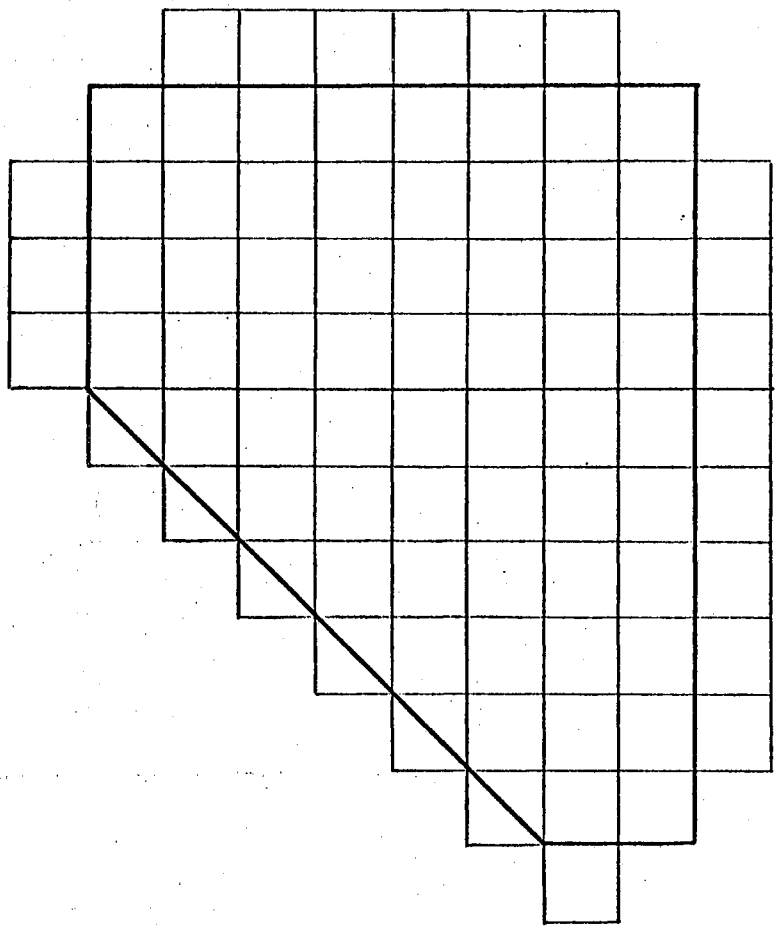

Figure 3. Fine Grid

shown tabulated in Figure 5 for subsequent use. Forces and moments were summed and found to be in equilibrium.

Airy Stress Function Construction

The form of the Airy Stress Function used in this analysis was the polynomial,

$$\Phi = \frac{1}{2} Ax^2 + Bxy + \frac{1}{2} Cy^2 + Dx + Ey + F . \qquad (2)$$

Stresses were integrated twice, and the constants D, E, and F were selected for each boundary segment to maintain continuity of the Airy function and its first partial derivatives at boundary nodes. Initial values of the arbitrary constants were assumed to be zero at the origin. The integration processes were calculated on an IBM 360/75. Table I shows the input for the calculations. The symbols A, B, and C are the stresses on the line segment under integration. The lower limit is the X and Y on the same line. The upper limit is the next point in the direction of line integration. Table II is the corresponding output. Column "Phi" is the Airy function at the point (n). On the same line, the slopes $\partial\Phi/\partial x$ and $\partial\Phi/\partial y$ are given for the point (n + 1). At point 9, for example, Φ = -25.3, and the slopes are $\partial\Phi/\partial x$ = 2.50 and $\partial\Phi/\partial y$ = -10.2.

Similar tables were obtained for line integration that proceeds clockwise. The residual Φ represents the cumulative error in line integration. Slope residuals were found to be negligible, assuring force equilibrium in the coordinate directions.

It is recommended that the boundary phi's be corrected before

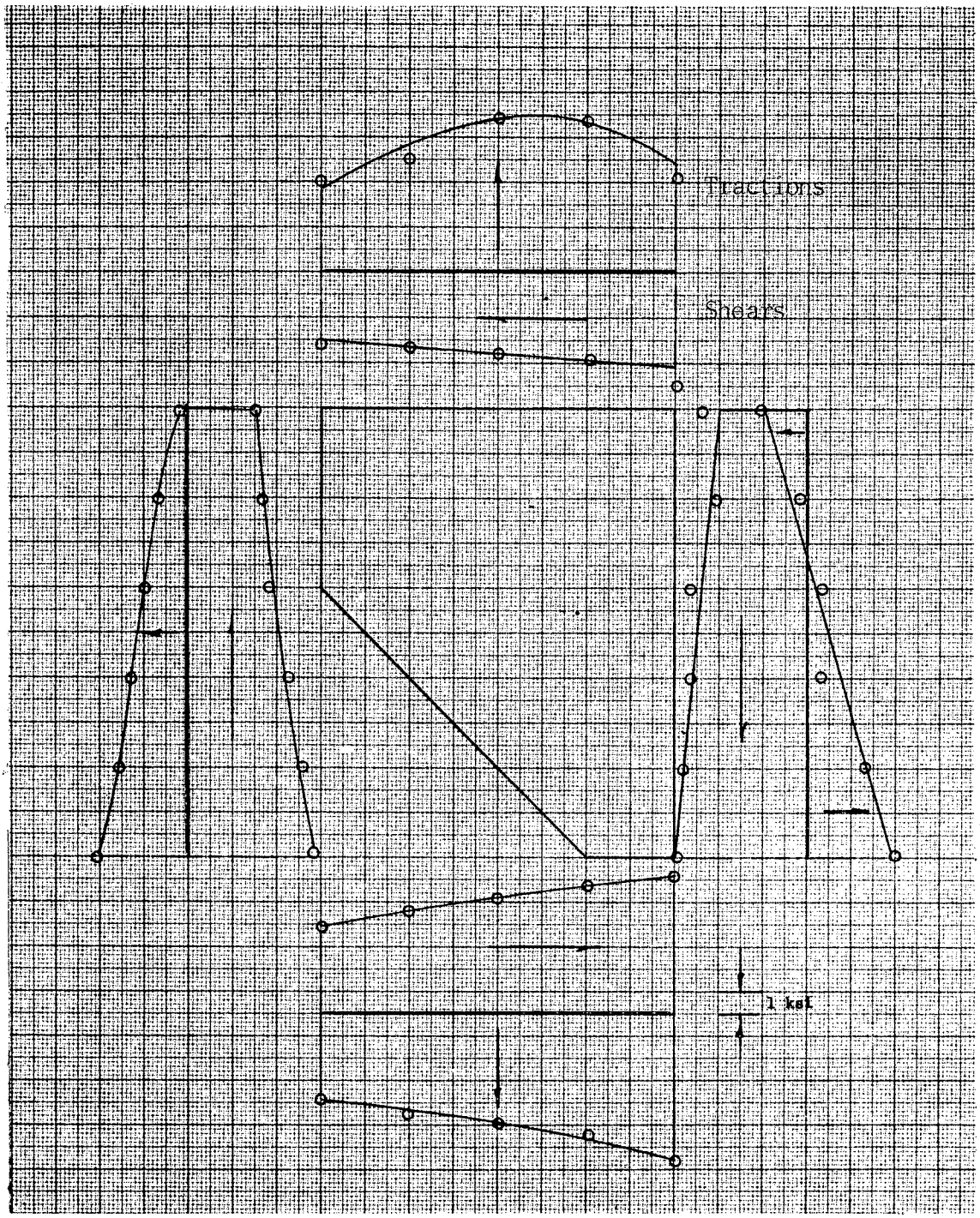

Figure 4. Boundary Shears and Tractions

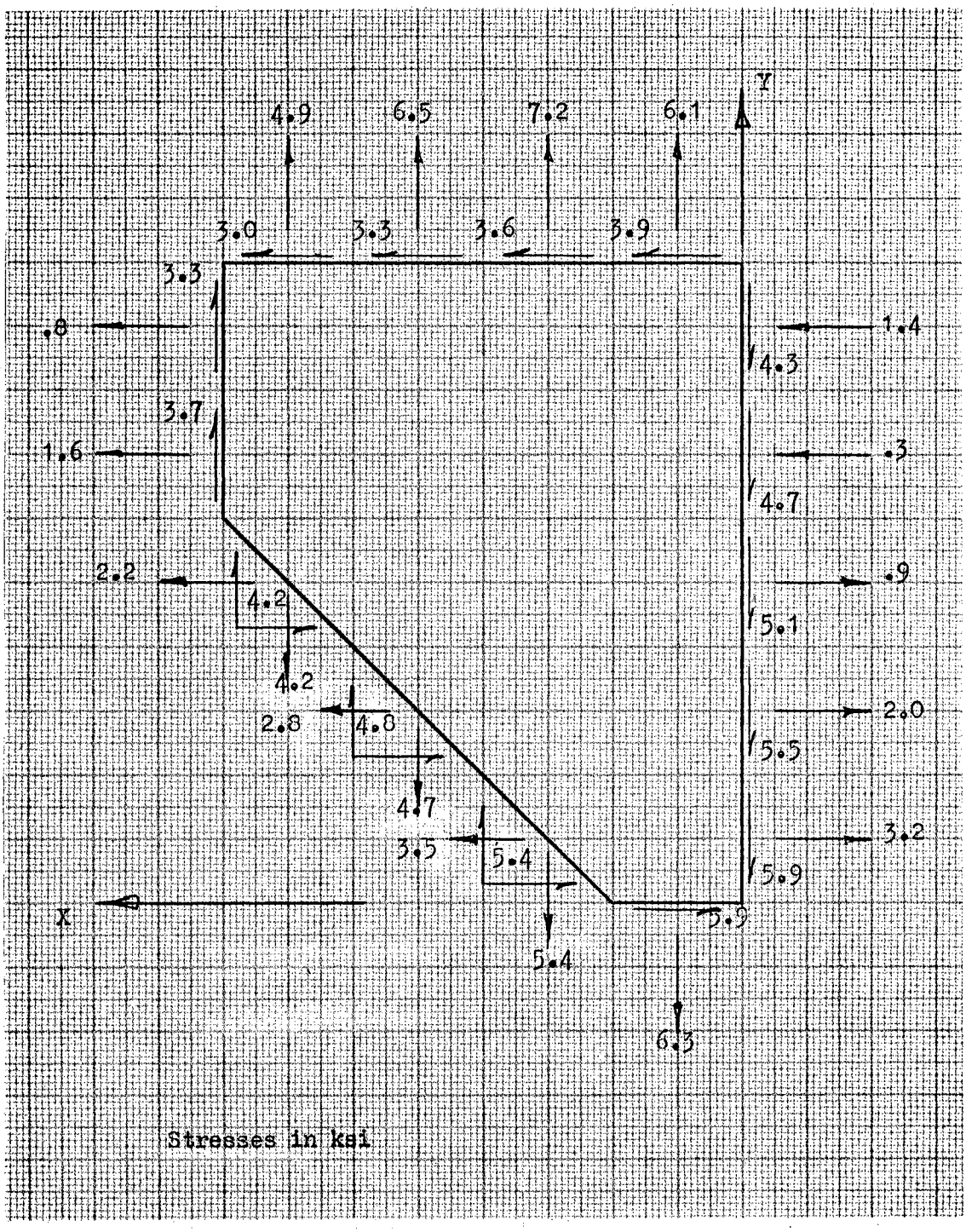

Figure 5. Boundary Stresses - Coarse Grid

TABLE I

BOUNDARY VALUE INTEGRATION - CLOCKWISE COARSE INPUT

A	B	C	X	Y	P	N
6.300	-5.900	0.0	0.0	0.0	1.000	1
5.400	-5.400	0.0	1.0	0.0	1.000	2
0.0	-5.400	3.500	2.0	0.0	1.000	3
4.700	-4.800	0.0	2.0	1.0	1.000	4
0.0	-4.800	2.800	3.0	1.0	1.000	5
4.200	-4.200	0.0	3.0	2.0	1.000	6
0.0	-4.200	2.200	4.0	2.0	1.000	7
0.0	-3.700	1.600	4.0	3.0	1.000	8
0.0	-3.300	0.800	4.0	4.0	1.000	9
4.900	-3.000	0.0	4.0	5.0	1.000	10
6.500	-3.300	0.0	3.0	5.0	1.000	11
7.200	-3.600	0.0	2.0	5.0	1.000	12
6.100	-3.900	0.0	1.0	5.0	1.000	13
0.0	-4.300	-1.400	0.0	5.0	1.000	14
0.0	-4.700	-0.300	0.0	4.0	1.000	15
0.0	-5.100	0.900	0.0	3.0	1.000	16
0.0	-5.500	2.000	0.0	2.0	1.000	17
0.0	-5.900	3.200	0.0	1.0	1.000	18

TABLE II

BOUNDARY VALUE INTEGRATION - CLOCKWISE COARSE OUTPUT

n	ϕ	$\left(\frac{\partial \phi}{\partial x}\right)$	$\left(\frac{\partial \phi}{\partial y}\right)$
1	0.315E 01	0.630E 01	-0.590E 01
2	0.121E 02	0.117E 02	-0.113E 02
3	0.260E 01	0.630E 01	-0.780E 01
4	0.112E 02	0.110E 02	-0.126E 02
5	0.500E-01	0.620E 01	-0.980E 01
6	0.835E 01	0.104E 02	-0.140E 02
7	-0.455E 01	0.620E 01	-0.118E 02
8	-0.155E 02	0.250E 01	-0.102E 02
9	-0.253E 02	-0.800E 00	-0.940E 01
10	-0.221E 02	-0.570E 01	-0.640E 01
11	-0.131E 02	-0.122E 02	-0.310E 01
12	0.265E 01	-0.194E 02	0.500E 00
13	0.251E 02	-0.255E 02	0.440E 01
14	0.200E 02	-0.212E 02	0.580E 01
15	0.141E 02	-0.165E 02	0.610E 01
16	0.840E 01	-0.114E 02	0.520E 01
17	0.420E 01	-0.590E 01	0.320E 01
18	0.260E 01	0.143E-04	0.763E-05

integration. Slope residuals were found to be negligible, assuring force equilibrium in the coordinate directions.

It is recommended that the boundary phi's be corrected before proceeding to the simultaneous equation formulation. A suggested method is shown in Table III. This method could be interpreted geometrically as "Airy Surface" tilting. Results of the correction procedure are tabulated in Figure 6. The Airy stress function calculations were made for the fine grid boundary locations in the same manner and the results are tabulated in Figure 7. These values and the slopes normal to the boundary are used to complete the formulation of the simultaneous algebraic equations.

The set of simultaneous equations can be obtained by writing one equation for each node. Successive application of the thirteen point biharmonic operator furnishes nine equations of the form,

$$20\Phi_0 - 8(\Phi_1 + \Phi_2 + \Phi_3 + \Phi_4)$$

$$+ 2(\Phi_5 + \Phi_6 + \Phi_7 + \Phi_8) + \Phi_9 + \Phi_{10} + \Phi_{11} + \Phi_{12} = 0. \qquad (3)$$

Important steps in the derivation of Equation (3) are given by Shaw [5].

Two methods are available for the fictitious point equation formulation:

$$\Phi_F = \Phi_R + 2\delta\left[\frac{\partial\Phi}{\partial x}\right]_B \qquad \text{"Two-Mesh"} \qquad (4)$$

$$\Phi_F = \Phi_B + \delta\left[\frac{\partial\Phi}{\partial x}\right]_B \qquad \text{"One-Mesh"} \qquad (5)$$

TABLE III

BOUNDARY PHI CORRECTION - COARSE GRID

Node	ϕ_{ccw}	ϕ_{cw}	$K_1 \phi_{ccw}$	$K_2 \phi_{cw}$
26	0		0	
36	1.60		1.53	
46	5.80		5.53	
56	11.40		10.87	
66	17.4		16.59	
76	22.4		21.36	
75	-.05		-.048	
74	-15.7		-14.97	
73	-24.7		-23.55	
72	-27.9	-25.3	-26.60	-26.60
62		-15.5		-16.30
52		-4.55		-4.78
42		8.35		8.78
43		-.05		-.053
33		11.2		11.78
34		2.60		2.73
24		12.1		12.72
25		3.15		3.31

$$K_1 = \frac{26.6}{27.9} \qquad K_2 = \frac{26.6}{25.3}$$

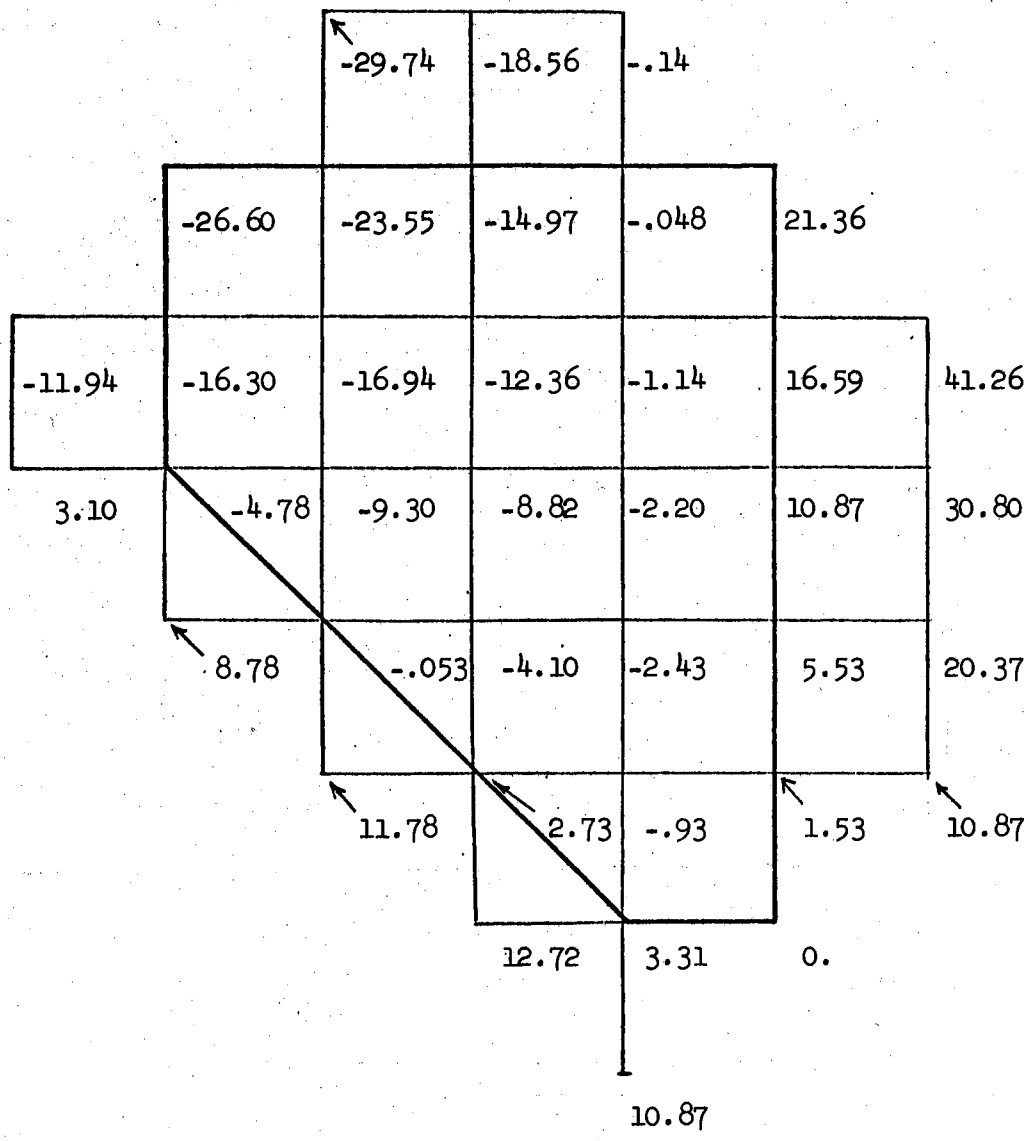

Figure 6. Airy Function - Coarse Grid

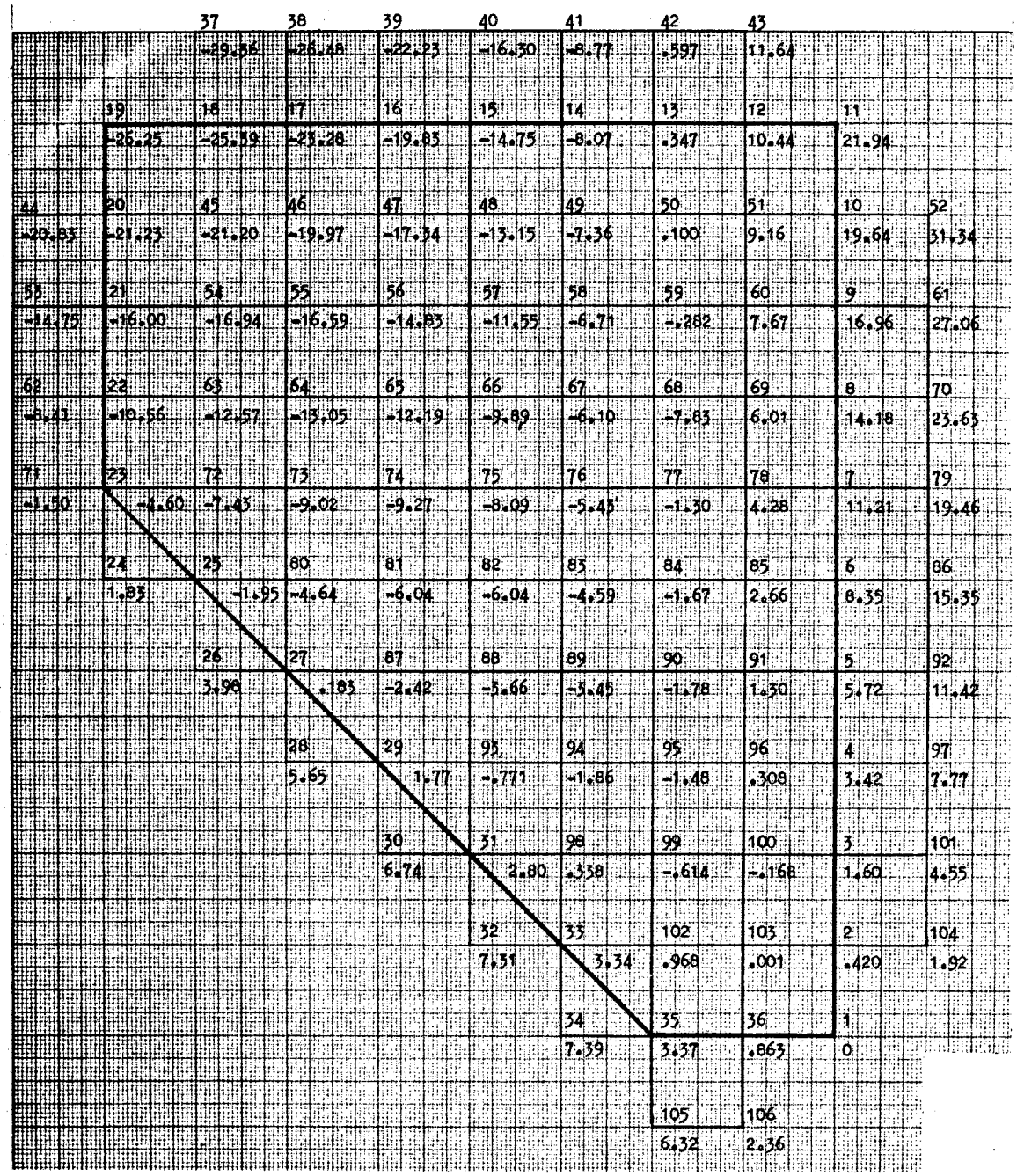

Figure 7. Airy Function - Fine Grid

The names "One-Mesh" and "Two-Mesh" are alternate methods of approximating fictitious values. Both approximations were used for fine and coarse grids, resulting in four variations of the Airy Matrix. For the coarse net, equations of this type furnished the required thirteen expressions for the fictitious points.

If selvedge points had been encountered, they could have been calculated with equation (6) suggested by Shaw [5];

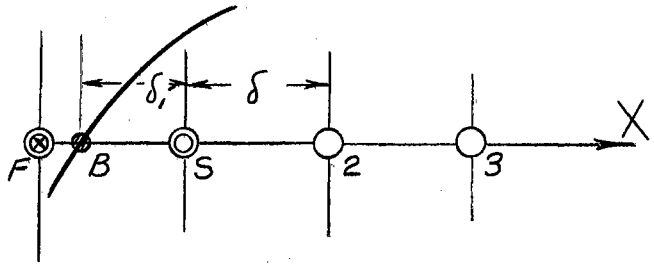

$$\Phi_S = E_4\ \Phi_B + F_4\ \Phi_2 - G_4\ \Phi_3 + H_4\,\delta\left[\frac{\partial\Phi}{\partial x}\right]_B . \tag{6}$$

The corresponding fictitious point equation would be;

$$\Phi_F = A_4\,\Phi_B + B_4\ \Phi_2 - C_4\ \Phi_3 - D_4\ \delta\left[\frac{\partial\Phi}{\partial x}\right]_B . \tag{7}$$

Expressions for the fictitious and selvedge points of the type (6) and (7) can be formed by extracting the constants from tables in Shaw's book for known values of the ratio,

$$a = \frac{\delta_1}{\delta} . \tag{8}$$

Boundary values are introduced as trivial equations of the form,

$$\Phi_B = \text{a constant}, \tag{9}$$

to simplify the stress calculations to follow.

For the coarse grid, 37 equations resulted; 106 equations resulted from the fine grid. The matrix of coefficients and the righthand side vector is illustrated in Table IV for the "Two-Mesh" coarse matrix.

Solutions were obtained for each of the 4 matrices on an IBM 360/75 using the Boeing Matrix Package [6].

Numerical values of the calculations thus obtained were transcribed on the nodal diagrams. The Airy "phi's" for the "Two-Mesh" coarse and "One-Mesh" fine grids are illustrated in Figures 6 and 7.

Stress Calculations

With the Airy values known everywhere, theoretical stress values may be calculated with the finite difference equations for stresses;

$$\sigma_x \approx \frac{\Phi_2 - 2\Phi_0 + \Phi_4}{\delta^2},$$

$$\sigma_y \approx \frac{\Phi_1 - 2\Phi_0 + \Phi_3}{\delta^2}, \tag{10}$$

$$\tau_{xy} \approx -\frac{(\Phi_5 - \Phi_6 + \Phi_7 - \Phi_8)}{4\delta^2}.$$

Derivation of these expressions are given in the book by Allen [3].

TABLE IV

AIRY MATRIX

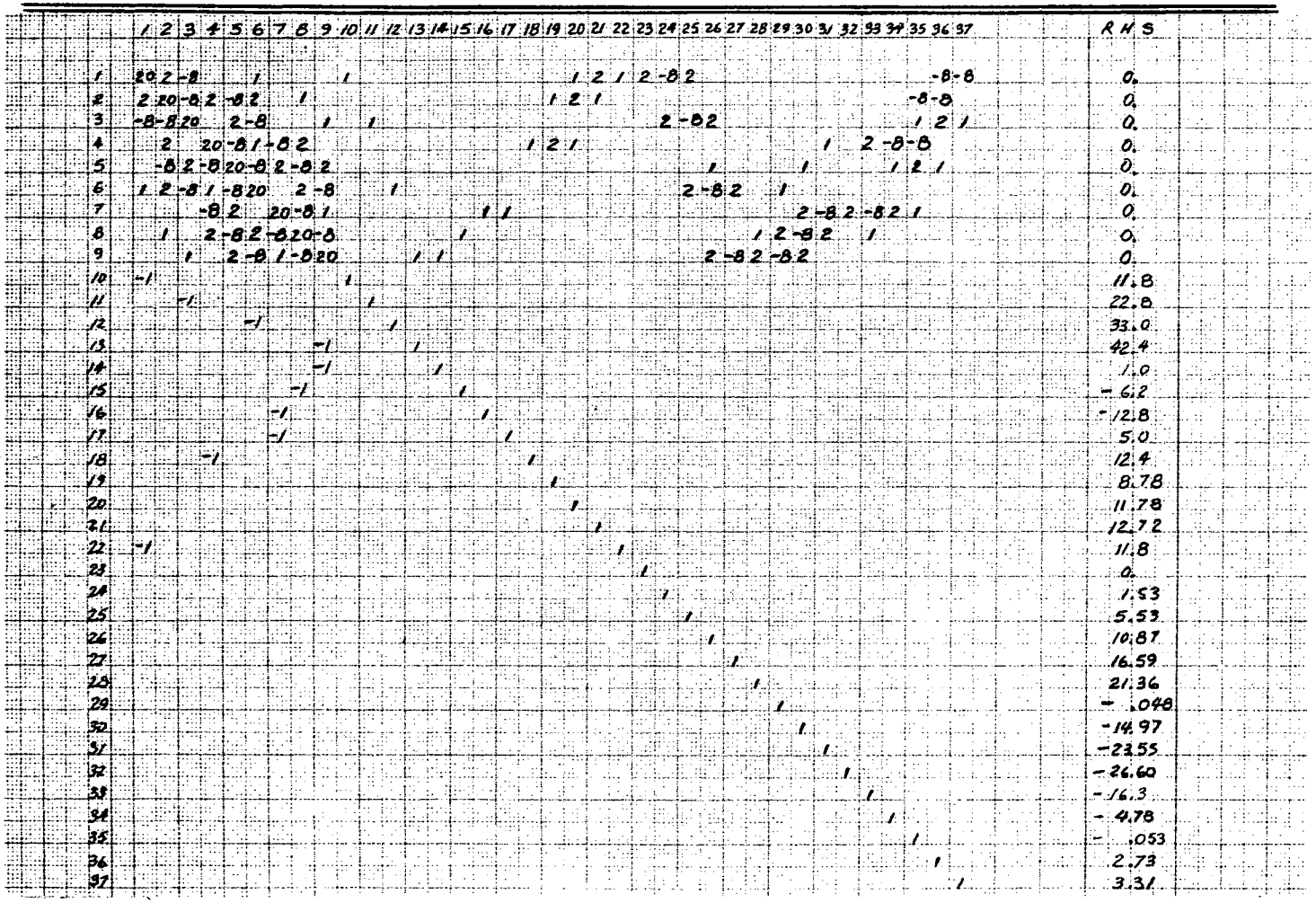

	1	2	3	4	5	6	7	8	9	10	11	12	13	14	15	16	17	18	19	20	21	22	23	24	25	26	27	28	29	30	31	32	33	34	35	36	37	RHS
1	20	2	-8		1				1										1	2	1	2	-8	2											-8	-8			0.
2	2	20	-8	2	-8	2		1											1	2	1														-8	-8			0.
3	-8	-8	20		2	-8			1		1													2	-8	2									1	2	1		0.
4		2		20	-8	1	-8	2										1	2	1								1		2	-8	-8						0.
5		-8	2	-8	20	-8	2	-8	2																1			1			1	2	1					0.
6	1	2	-8	1	-8	20		2	-8		1													2	-8	2		1										0.
7			-8	2		20	-8	1						1	1														2	-8	2	-8	2	1				0.
8		1		2	-8	2	-8	20	-8				1															1	2	-8	2		1					0.
9			1		2	-8	1	-8	20			1	1												2	-8	2	-8	2										0.
10	-1									1																												11.8
11			-1								1																											22.8
12					-1							1																										33.0
13							-1						1																									42.4
14							-1							1																								1.0
15								-1							1																							-6.2
16							-1									1																						-12.8
17							-1										1																					5.0
18				-1														1																				12.4
19																			1																			8.78
20																				1																		11.78
21																					1																	12.72
22	-1																					1																11.8
23																							1															0.
24																								1														1.53
25																									1													5.53
26												1														1												10.87
27																											1											16.59
28																												1										21.36
29																													1									-.048
30																														1								-14.97
31																															1							-23.55
32																																1						-26.60
33																																	1					-16.3
34																																		1				-4.78
35																																			1			-.053
36																																				1		2.73
37																																					1	3.31

Since the biharmonic operator ("thirteen point star") has its x-axis directed to the left, the cyclic node numbering is clockwise as shown. When the phi data are transcribed as shown in Figure 7, it is convenient to prepare a window template (tic-tac-toe) so that erroneous data will not be used. It is suggested that this template be drafted on a sheet of vellum paper, as shown in the sketch.

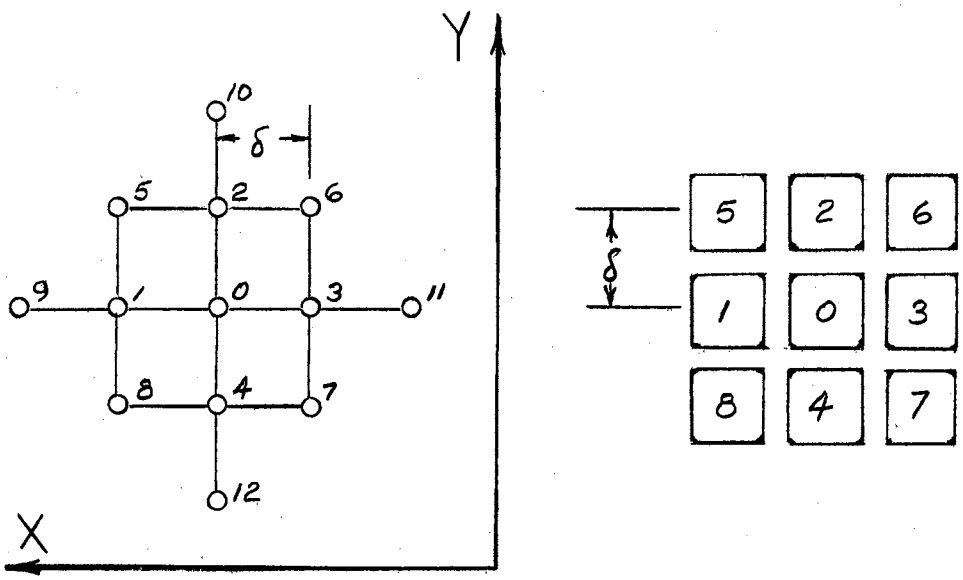

Stress calculations were carried out for several points to provide the desired theoretical-to-experimental correlation. The stress equations (10) were programmed and calculated on the IBM 360/75. A sample input for a horizontal and vertical cross section is illustrated in Table V. Corresponding output of analytical values of stress is presented in Table VI. These data are plotted for theoretical-to-experimental comparison.

TABLE V

AIRY FUNCTION - "TWO-MESH" COARSE GRID

NODE	1 ϕ_0	2 ϕ_1	3 ϕ_2	4 ϕ_3	5 ϕ_4	6 ϕ_5	7 ϕ_6	8 ϕ_7	9 ϕ_8
74.0	-14.97	-23.55	-18.56	-.048	-12.36	-29.74	-.14	-1.14	-16.94
64.0	-12.36	-16.94	-14.97	-1.14	-8.82	-23.55	-.048	-2.20	-9.30
54.0	-8.82	-9.30	-12.36	-2.20	-4.10	-16.94	-1.14	-2.43	-.053
44.0	-4.10	-.053	-8.82	-2.43	2.73	-9.30	-2.20	-.93	11.78
53.0	-9.30	-4.78	-16.94	-8.82	-.053	-16.30	-12.36	-4.10	8.78
55.0	-2.20	-8.82	-1.14	10.87	-2.43	-12.36	16.59	5.53	-4.10
56.0	10.87	-2.20	16.59	30.80	5.53	-1.14	41.26	20.37	-2.43

TABLE VI

STRESS CALCULATIONS - "TWO-MESH"
COARSE GRID

Node	Sigma XX	Sigma YY	Tau XY
74	-0.980	6.342	-3.450
64	0.930	6.640	-4.100
54	1.180	6.140	-4.544
44	2.110	5.717	-4.952
53	1.607	5.000	-4.205
55	0.830	6.450	-4.830
56	0.380	6.860	-4.900

These stresses are compared to experimental data in Figure 16.

An Alternate Analysis Method

An alternate analysis, the "Direct Stiffness Method" of Turner, et al. [7], was also used to calculate stresses. Pairs of equivalent nodal forces were assigned as shown in Figure 8. The structure was idealized as fourteen rectangular elements and three triangular plate elements. Analysis of the assemblage was accomplished with the Boeing computing programs. Results are shown in Figure 9. The stresses were obtained for comparison with the finite difference method and the experimental data.

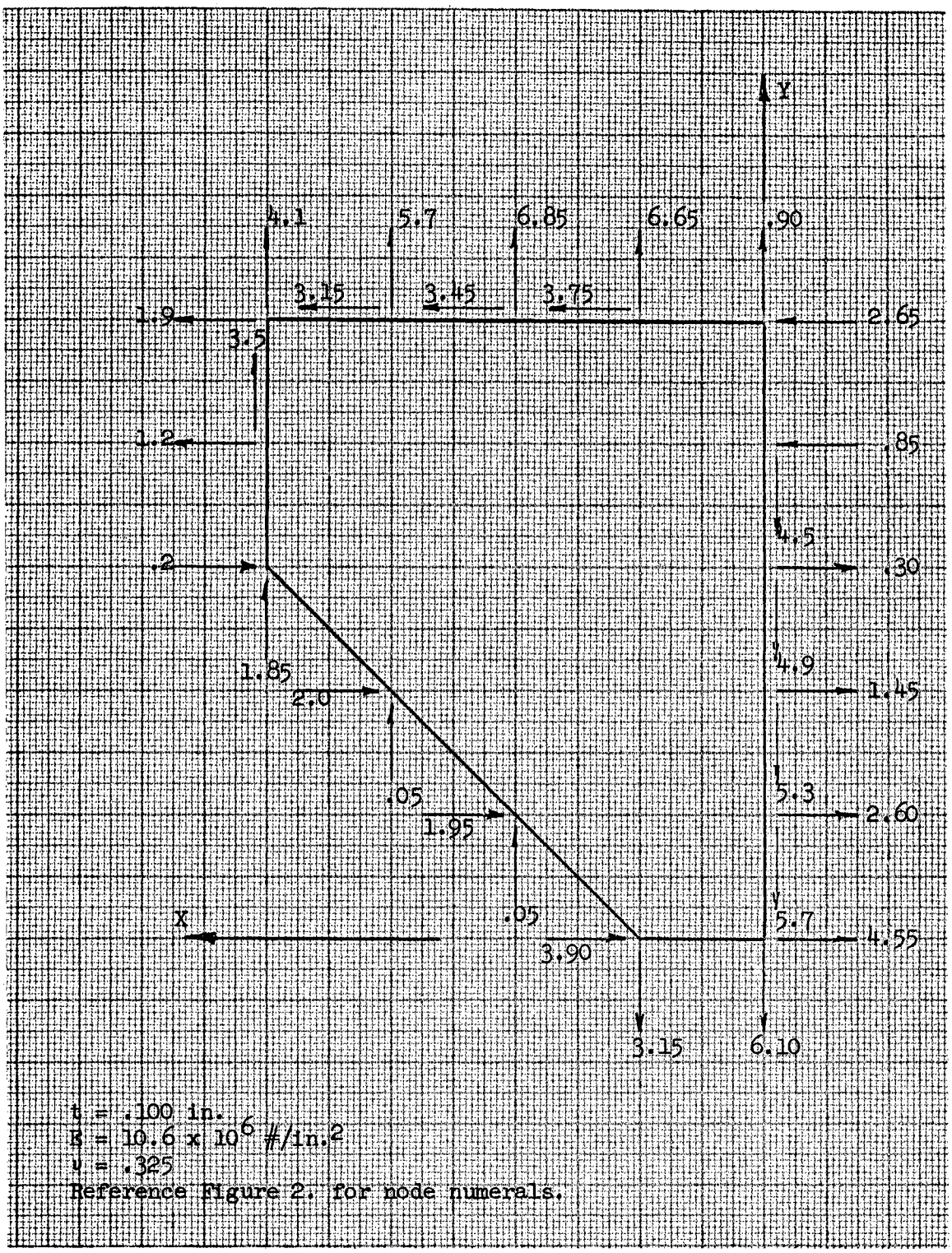

Figure 8. Equivalent Nodal Forces

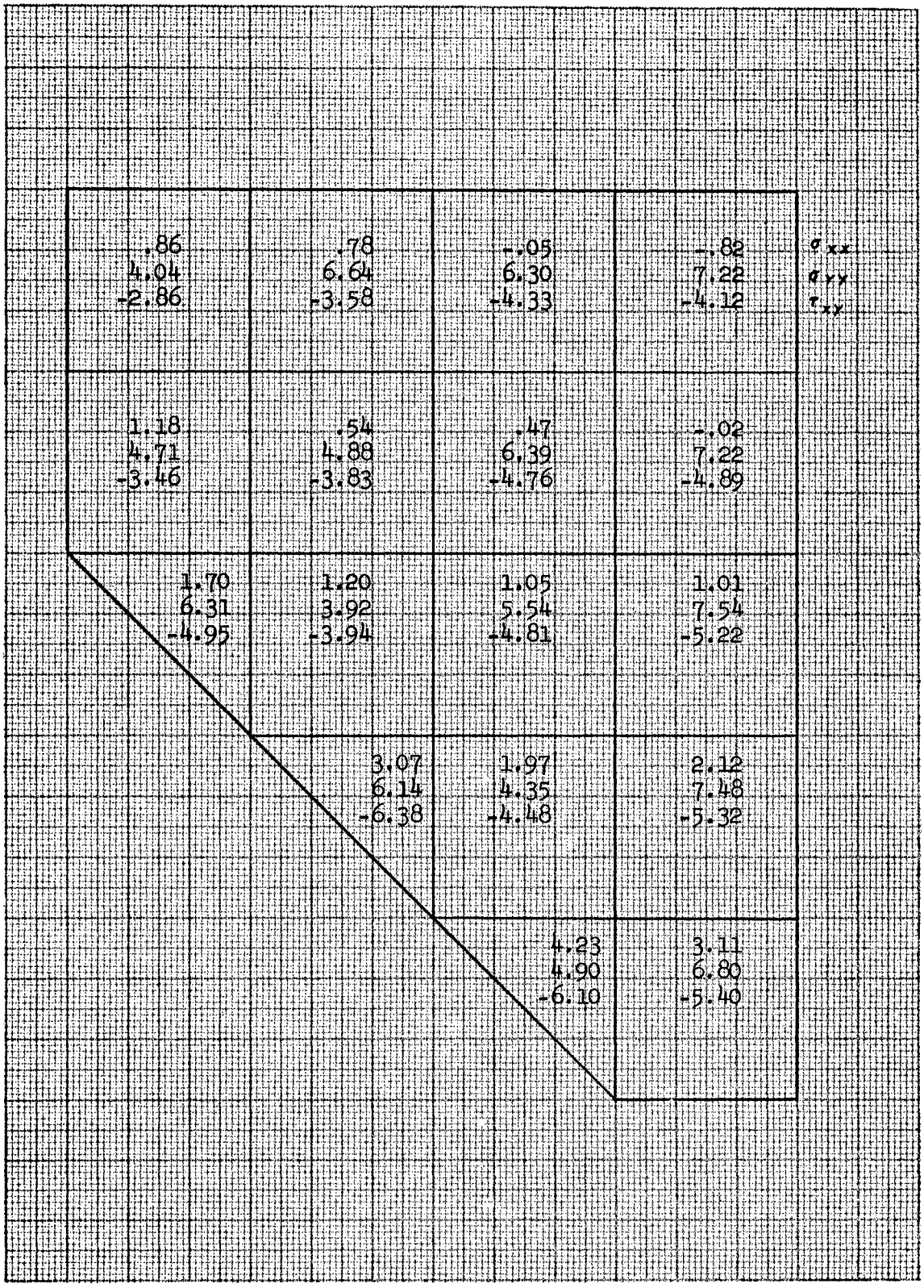

Figure 9. Stress Calculation Results - Direct Stiffness Method

CHAPTER III

EXPERIMENT

This chapter contains a description of the experiment which was conducted to substantiate the validity of the proposed method of analysis. The test specimen, test loads, measuring equipment, and resulting data are described. The experiment superficially resembled an aircraft static test in miniature proportions. It is fitting to describe the experiment as one in the field of two-dimensional elastostatics. Experimental information of the type described in this document is not available in the published literature.

Information in this chapter is arranged into subparts as follows:

Specimen Selection (Purpose of Experiment)

Specimen Description

Loading Apparatus

Strain Instrumentation

Indicating and Recording Equipment

Experimental Procedure

Experimental Data

Comparison of Results

Ancillary Experiments

Specimen Selection

The purpose of the experiment was to provide experimental evidence to substantiate the method of analysis previously described. Since the desired analysis method is applicable to a two-dimensional region of arbitrary external boundary, the experimental criteria are stringent. The specimen must have at least one curved boundary, and at least one boundary with distributed loads.

The specimen must also conform to the restrictions placed on the theoretical analysis. The test region must have plane stresses, must not be loaded beyond its elastic limit, and must not be allowed to wrinkle. On the other hand, the stresses imposed must be high enough to avoid error in relative magnitude of strain sensitivity and measured strain signal. Data from a specimen having this degree of complication are not available in the published literature.

Specimen Description

The specimen was a newly designed structural article described in Boeing Drawing 35-26401 [8]. A perspective drawing is included as Figure 1. Figures 10 and 11 are photographs of the specimen. The test specimen and the test jig are shown in Figure 12. The structure is an externally stiffened semi-monocoque cylinder of aluminum alloy construction, 30" in diameter and 48" long. It has an aluminum stiffened bulkhead at the test end, two intermediate frames, and a steel ring and plate adapter at the jig ("live") end. Aircraft quality materials and manufacturing methods were used throughout, except that simplifications and material substitutions were allowed when the data zone was not compromised. Figure 10 is an external view of the structure.

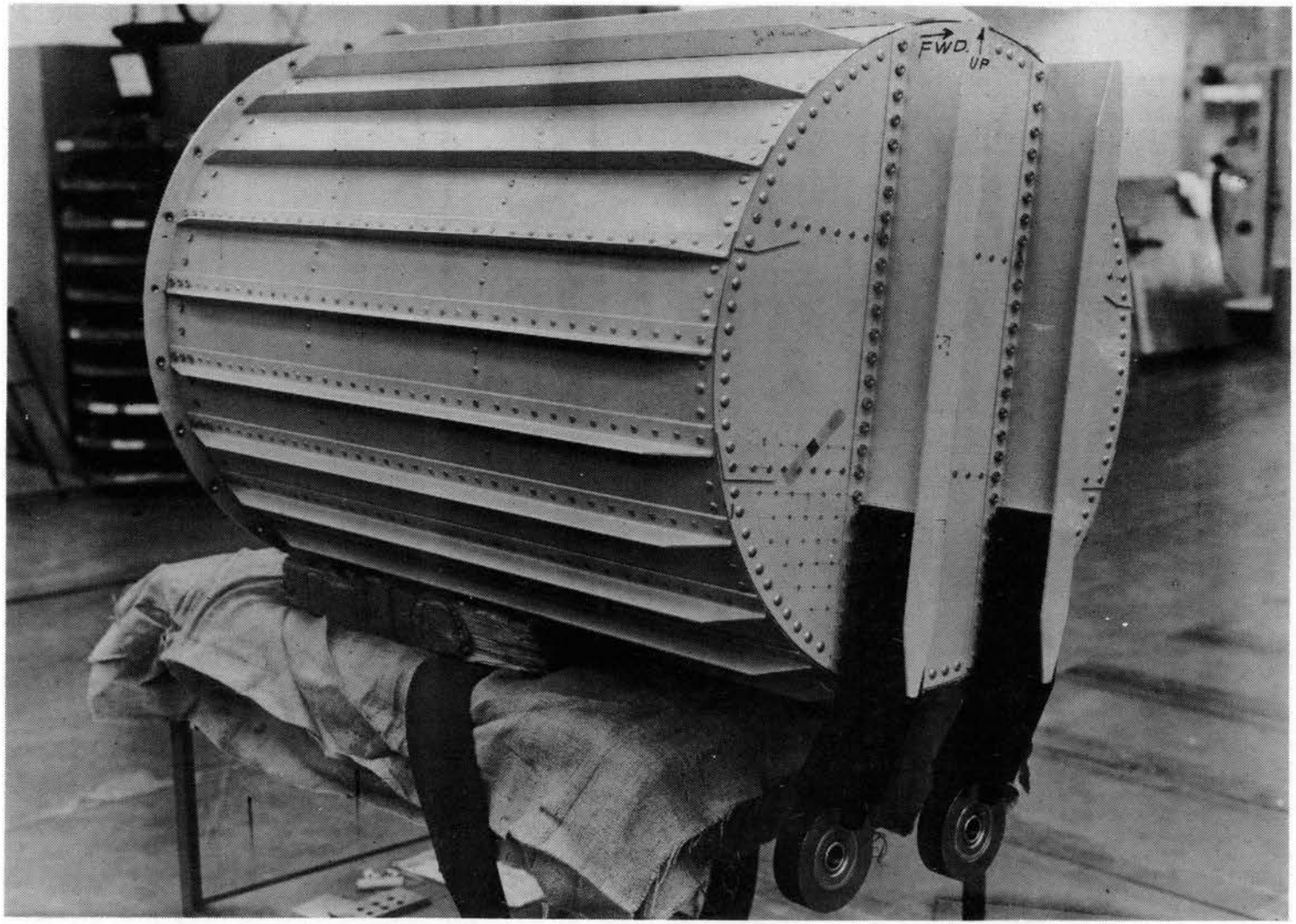

Figure 10. Experimental Specimen - External View

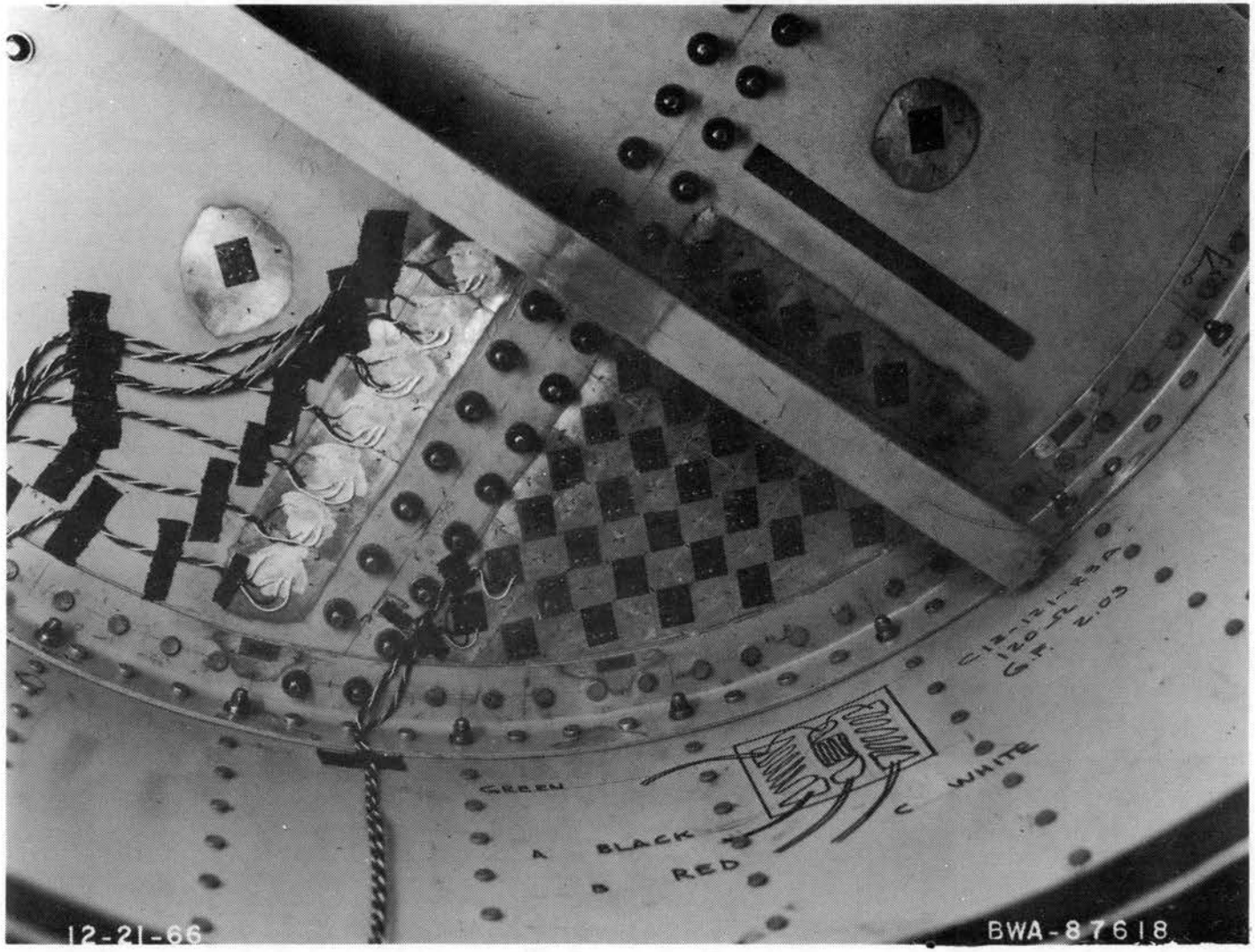

Figure 11. Test Region - Internal Close-Up

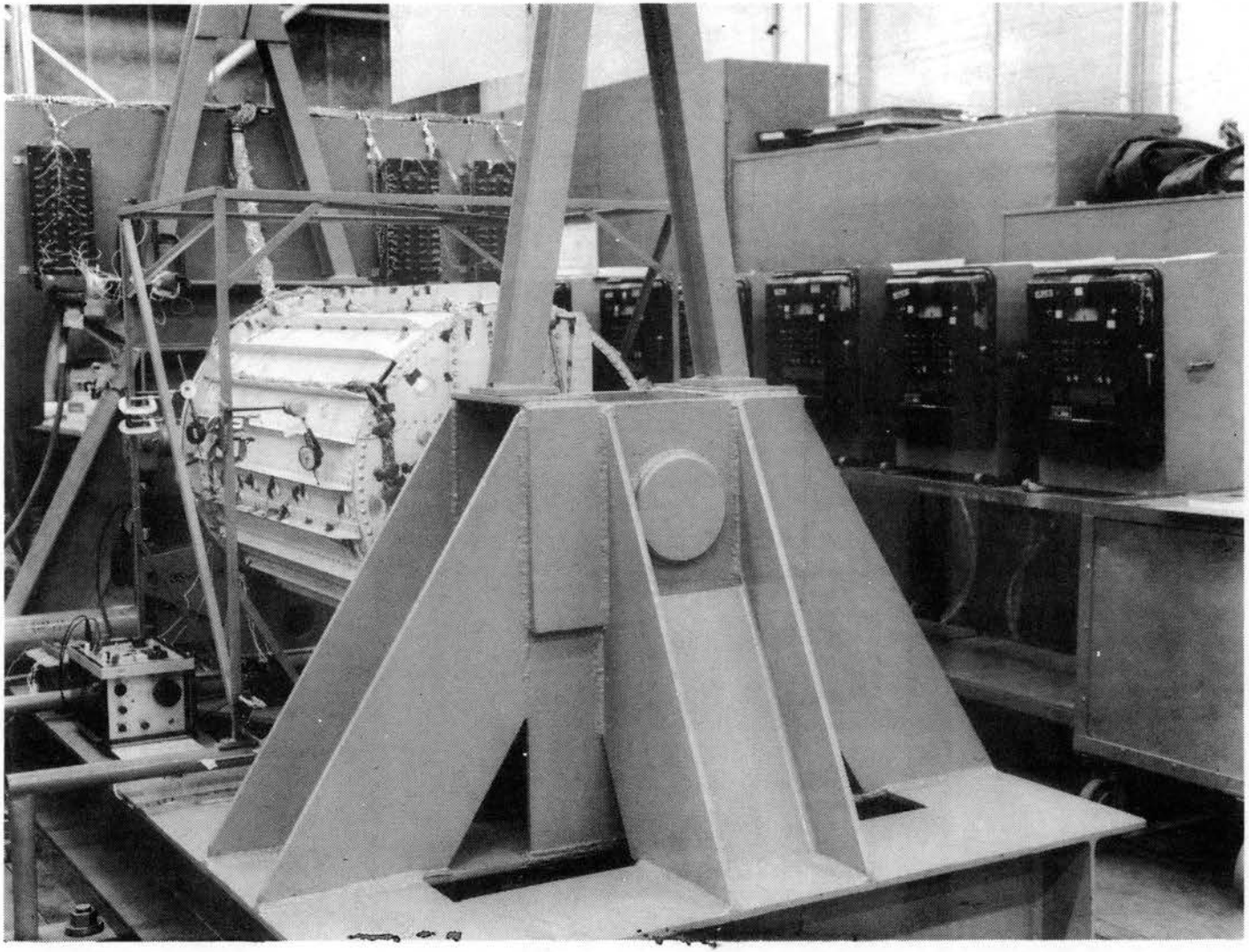

Figure 12. Experimental Arrangement

Figure 11 is an internal view of the bulkhead web.

The cylinder functions to provide the desired elastic support and distributed stresses on the curved edge of the test zone. Cylinder length is desired to allow a uniform shear flow at the jig end and imposed stress in the vicinity of the bulkhead.

It was hypothesized that the shear flow at a station close to the bulkhead would not be uniform as predicted by the elementary formula. It was believed that the bulkhead stiffness influences the local distribution of loads in the skin. Although the success of the experiment was not dependent on the stress redistribution, provision was made for it.

The cylinder, stiffeners, frames, and supporting equipment have been purposely designed overstrength to insure elastic behavior by the "boundary structure". The test zone material is 2024-T351 aluminum alloy, .100" thick. The straight boundaries are aluminum extrusion, and the curved boundary is a formed aluminum angle which provides a shear transfer path to the cylinder shell skin. The stiffeners are of realistic proportions to prevent buckling of the curved skin. The two formed frames are much heavier than is required in aircraft. They were designed to provide stability for the stiffeners.

It was planned to apply a pure torsion load at the jig end and react with a "pure couple" at the test end. For this reason, the fittings at the test end were designed to eliminate extraneous side loads. A slotted bearing plate and special bolts with double flats allowed lateral translatory freedom. The friction component was minimized by strict requirements on the sliding surface and by aircraft quality dry lube surface treatment. Induced torsion could have been partially

reacted by a horizontal couple resulting from side load at the fittings and the side bending stiffness of the cylinder.

Plane stress in the bulkhead web was a design requirement and was satisfied by placing the theoretical centerline of the self-aligning bearing in the theoretical centerplane of the bulkhead web. The offset blade on the terminal fitting was necessary to carry the direct load from the bearing, through the bearing housing and splice plates to the webs of the vertical coaming members. The double row self-aligning roller bearings allowed for installation alignment precision. They are the largest of the "C Series" and were furnished by the Shafer Division of Rex Chainbelt Company.

Load transfer from the vertical coaming was accomplished with two rows of high strength, close tolerance bolts. The actual load per bolt diminished with distance from the fitting end, as it does in an actual aircraft structure. Bolt load distribution was incidental except that the complication of realism was necessary and desirable as a critical basis for the proposed analysis. Determination of the distribution by theoretical means was not a part of this investigation. Measured values of resulting stresses in the test membrane are considered to be the "known" boundary stress condition.

Universal head aluminum rivets were used for stiffener-to-skin attachments, frame-to-skin attachments, and bulkhead ring to bulkhead web attachments. Taper shank bolts were used at locations where tensile components may result, such as the stringer-frame juncture and extrusion end points. High strength steel fasteners were also used where shear flows warranted it, such as at the horizontal stiffener-to-web attachment.

The jig end of the cylinder was attached to a commercial steel annular ring of angular cross section. The outside diameter of the cylindrical surface of the ring was designed to mate with the inside diameter of the cylindrical skin, allowing the skin and 24 stiffeners to be spliced with a single structural member.

Ring-to-disk bolts allowed for specimen installation and removal by completely external access to bolt heads and nuts. The steel disk merely adapted the specimen circular cross section to the jig rectangular end plate.

The disk, ring, and stiffener-to-ring attachments were designed for appreciable bending moment. Although a bending moment was not a planned loading condition, the specimen has inherent strength capability for future bending and compression experiments. Small bending components were unavoidable. They can arise from slight misalignment errors between the jig centerline and the theoretical centerline of the cylinder. Six 4" diameter holes are designed in the disk to provide access and space for strain gage wire bundles.

Loading Apparatus

The loading apparatus is described in Boeing Drawing 35-21491 [9]. It is a heavy, steel framework about 11 feet long, 6 feet wide and 4 feet high. The jig was designed and built by The Boeing Company, Wichita Division, during a company-sponsored research program on integral fuel tank sealants.

Pure torsion was obtained as shown schematically in Figure 13. A 5" diameter hydraulic ram load acting on a 6.5" moment arm induced axial loads in the push-pull rods. A load cell and turnbuckle included

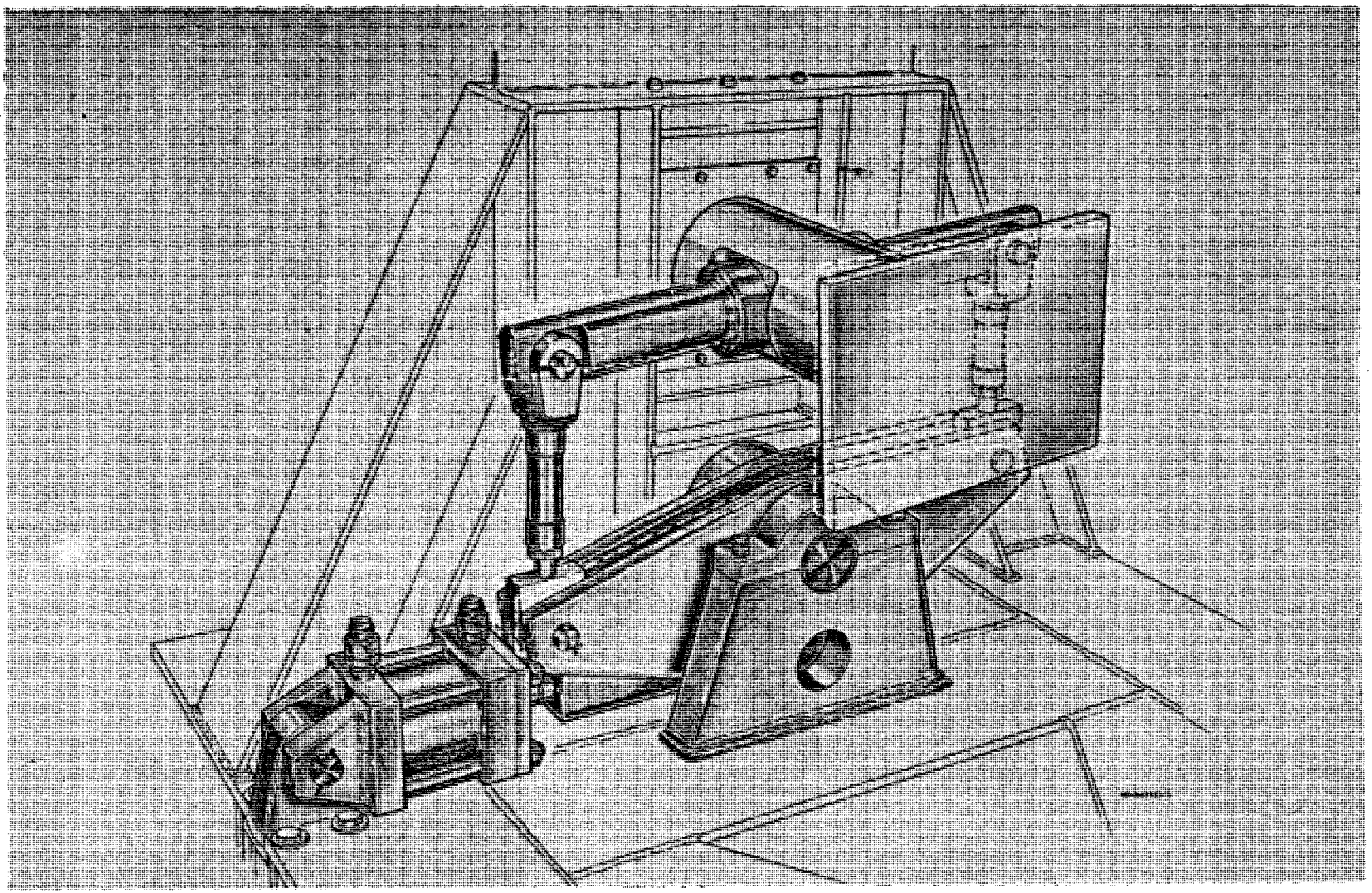

Figure 13. Hydraulic Torsion Mechanism

in each rod allowed precise adjustment and measurement of induced torsion. The push-pull rod acts on a double crank arm through the heavy torsion shaft. A rectangular plate welded to the shaft was intended to transmit the torsion to the integrally sealed fuel tanks. The circular disk of 35-26401 was fastened to the rectangular pad with fourteen 1/2" diameter steel bolts.

Strain Instrumentation

Strain measurements were essential to this research since they provided the necessary boundary and regional stress data to substantiate the proposed theoretical method. Bonded electrical resistance strain gages were the primary instruments for strain measurements.

A total of 116 rosettes and 73 axial gages were used to obtain 421 active channels of data. Twenty-six standards were also used for a total of 215 gages. The strain gage locations and types are shown on Boeing Drawing 35-26994 [10].

The zone of primary interest, Figure 11, contains the internal rosettes (type C12-121-R3A) and three axial gages (type C12-141-B). Many other details visible in this photograph are grid orientation, lead color loading, tinned tabs, gage lead anchors, gage waterproofing, and a 6" steel scale.

Indicating and Recording Equipment

Strain gage leads were gathered, bundled, and routed to a central point on the J-Box mounting board as illustrated in Figure 12. Cables

from twenty-six junction boxes were used to carry the strain signals to the indicating and recording equipment.

Eight Leeds and Northrup "Speedomax" Type G indicators were used to obtain the primary data from the rosettes in the high interest zone. The Gilmore Graphical Plotter, Model 114, was used to record the secondary strain data. Gilmore data were secondary but provided the extra channels to insure safety of the specimen and linear elastic behavior of the structural components. Highly stressed areas were carefully monitored during the test with the use of this equipment.

Experimental Procedure

The test specimen was completely designed, procured, manufactured, and gaged at The Boeing Company in Wichita. Two preliminary procedures were required prior to the execution of the major test: calibration of the load cells and slope setting on the strain indicators.

Each load cell in the jig was equipped with a full bridge and leads for recording. The load cells are the integral members in a vertical position between the rocker and the shaft crank pins illustrated in Figure 13. A turnbuckle nut with left- and right-threaded ends is provided for load equalization between the push-pull rods. The centerline dimension between load cells is 32 inches. For this couple distance, a 13,300 pound load was required to bring the specimen to its maximum design torque of 425,000 inch-pounds. Each load cell was removed from the jig and calibrated to 16,000 pounds to insure load linearity beyond the expected loading range. The east load cell was calibrated to 16,000 pounds tension at 2,000 pounds ascending increments and 4,000 pounds descending increments. The west load cell was calibrated

similarly to 16,000 pounds compression. Calibration curves for the two load cells are colinear and are shown in Figure 14.

The load cells were reinstalled in the jig and calibrated with shotbags on a 64" lever arm. A strain signal bias produced by the vertical shear component was removed by installing a machinist's jack during the calibration procedure. The percent load indicators were positioned and the load cell leads were connected. The maximum safe load was 66 percent, corresponding to 11,000 pounds average cell load, and the pressure gage dial reading was 5,000 psi.

The second preliminary procedure was the series calibrating the strain indicators. A precision decade box was used for each of the eight "Speedomax" units. The combinations of gage factor, resistance, and modulus of elasticity resulted in slope settings ranging from 39 to 42.

A similar procedure was used with the Gilmore Plotter, except that a decade box was not required. The 96 channels of data were grouped in four banks of 24 each. The slope setting on each of the four banks was "dialed in" with potentiometer controls on the face of the machine. Combinations that resulted in nearly equal slope settings were grouped together. Generally speaking, there were three major groupings: rosettes, metalfilm axials, and wire axials. It was convenient to group the rosettes into "high" and "low" resistance groups, 122.6 ohms and 121.6 ohms. Data were measured and recorded for each leg of each gage.

A double check was provided by constructing two cantilever beams: one of 4130 steel, the other of 2024 aluminum. Readings from these gages confirmed the settings with the potentiometers.

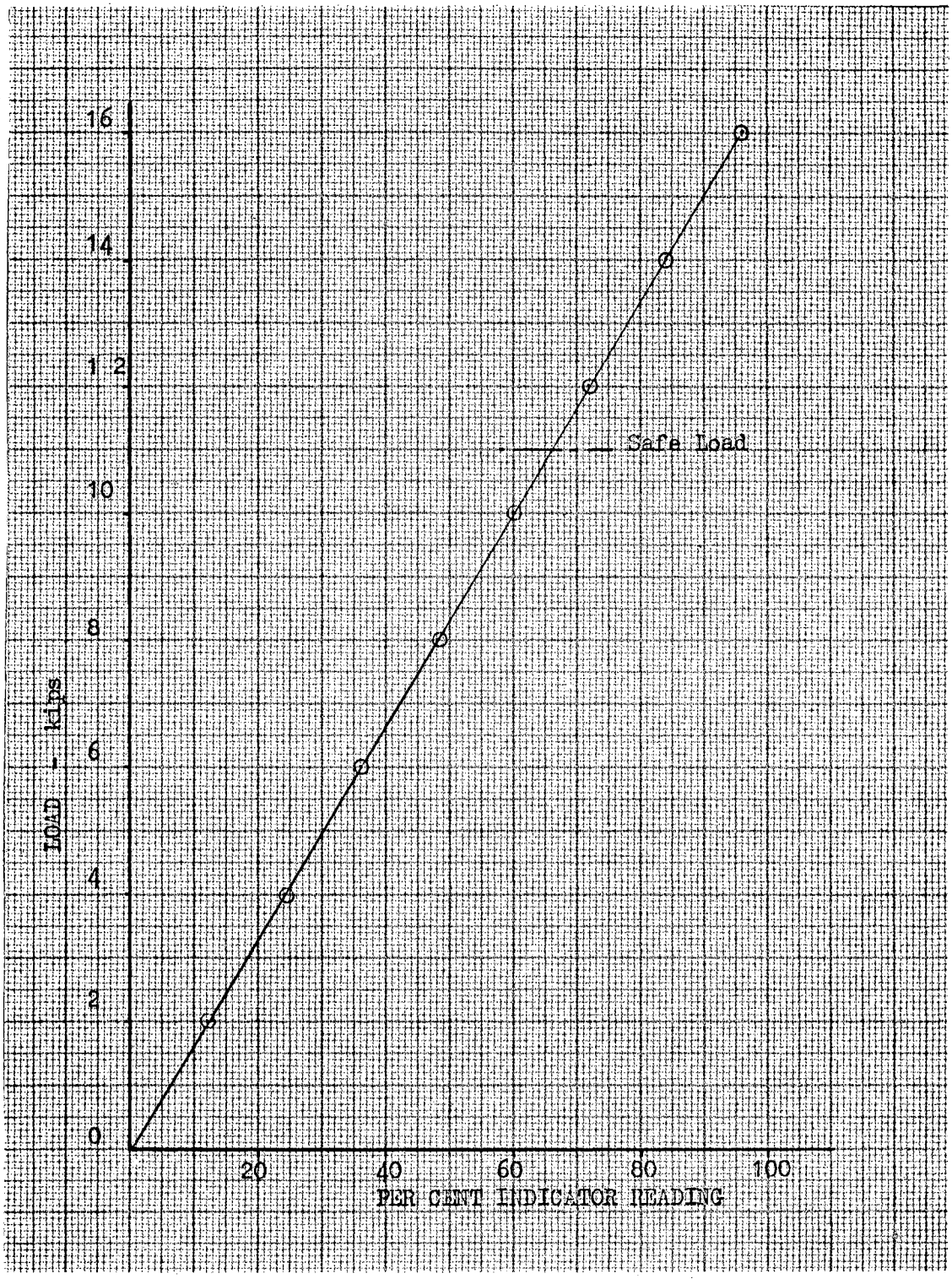

Figure 14. Load Cell Calibration Curves

The general arrangement during the major experiment is illustrated in Figure 12. The jig, specimen, and J-Boxes to the Gilmore are clearly seen. The original Baker hydraulic ram was used during the first test but was later replaced with a five-inch diameter Regent ram of comparable load capacity. The Baker ram, designed for cyclic loads, is equipped with metal seal rings which do not hold static load satisfactorily. The Regent ram is seen in the lower left of Figure 12. The Speedomax strainometers may be seen on the right. Two dial gages for deflection measurement and the space frame reference are also visible. The two cantilever beams are shown in the background fastened to the end of the jig. Two large "C" clamps and the small shotbags are visible.

The first major test series were run at zero, 24, zero, 48, and zero percent load cell calibration load. Data were recorded at 12% increments to 60% during the second experiment series. The final increment was 6% for a maximum of 66%. Values corresponding to 66% are: pressure, 5,000 psi; torque, 352,000 inch-pounds; and reaction load, 35,200 pounds.

The Regent ram was installed and used for the third series of tests. One hundred percent test load (66% ultimate) was applied nine times during the fourth series. Data were taken on trials 1, 2, 7, 8 and 9. These trials were planned as the "wringing-out" loadings, a procedure practiced by NASA, The Boeing Company, and reported by other companies. Preliminary data reduction and analysis revealed some questionable readings which were checked during the fifth series of tests. Load was applied and maintained during the "trouble-shooting".

During the sixth and final series, the entire test was repeated in the presence of several invited witnesses.

Experimental Data

Strain data in the region of high interest were assembled and averaged "back-to-back" for each leg and transcribed on input data sheets for digital computer solution of principal stresses and directions. The results are summarized in Figure 15. Maximum principal stress, minimum principal stress, maximum shear stress, and the direction of sigma one are tabulated at each node. At the lower right corner node, the maximum principal stress is 11.58 ksi and is inclined 38.6 degrees counterclockwise from vertical (a compass heading of 149.4^{o} from true north).

External forces derived from midplane stresses were in total equilibrium. The average strain dispersion for back-to-back rosettes was $\pm$14% for the 48 rosettes in the test region. The variation in strain was probably caused by the slight elastic buckle that was observed in the lower central web adjacent to the heavily instrumented zone. Data at coordinate node point 43, an anomaly, were not used. Interpolated values were used instead.

The principal stresses and directions were resolved about coordinate axes by rotations of the vectors. Values of outward normal stress and shear stresses on the boundary are plotted at the 15 boundary nodes, Figure 6. These were the stresses that were used in the subsequent theoretical Airy function construction.

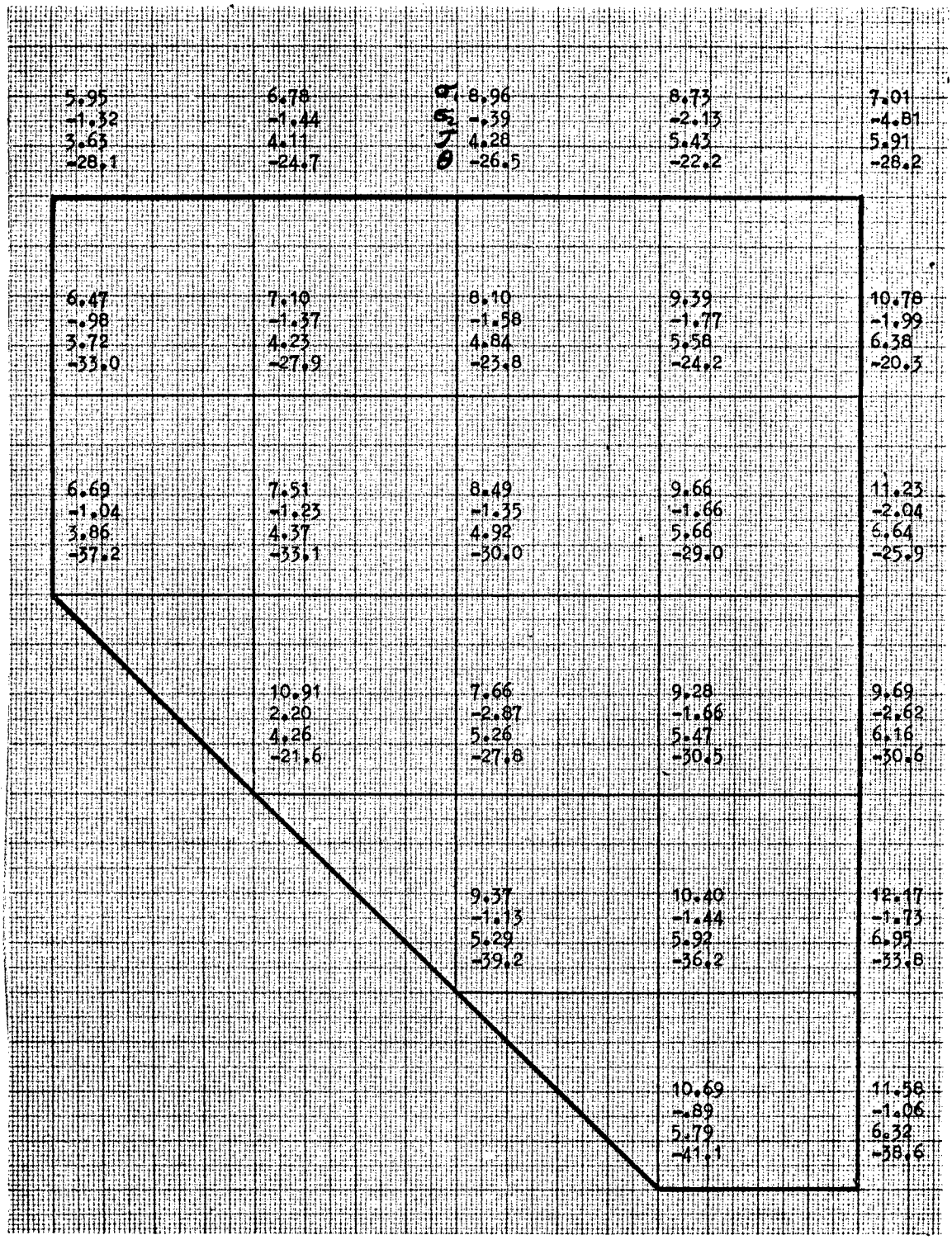

Figure 15. Experimental Stresses

Comparison of Results

Comparison of results showing theoretical and experimental stresses are shown in Figures 16 through 19. Theoretical stresses from the finite difference methods were overlayed on families of curves joining experimentally-measured points. Stress dispersion is indicated by a heavy vertical line from "stars" (analysis points) to the constructed continuous curves (experimental data). Direct examination of the graphical data is considered to be more meaningful than a percentage comparison because absolute values are often near zero. Agreement is seen to be near perfect (within $\pm$300 psi) for shear stresses, axial stresses in the x-direction, and certain y-direction stresses. Greatest dispersion is seen to occur in the axial stresses in the y-direction near the boundaries. Theoretical values were 1300 psi lower than measured values.

A similar comparison of the newly obtained experimental data with the alternate analysis method is shown in Figure 20.

Since the stresses for the direct stiffness method of analysis are assumed to act at the center of the plate, analytical values were compared to interpolated experimental values at corresponding points on the membrane. Correlation with the stiffness method, the finite difference method, and the newly obtained experimental data is seen to be excellent. This result was anticipated by the theoretical preliminary work by Chapel and Smith [11]. Stresses in a triangular plate element are difficult to interpret, and care should be taken when comparing calculated values with measured values.

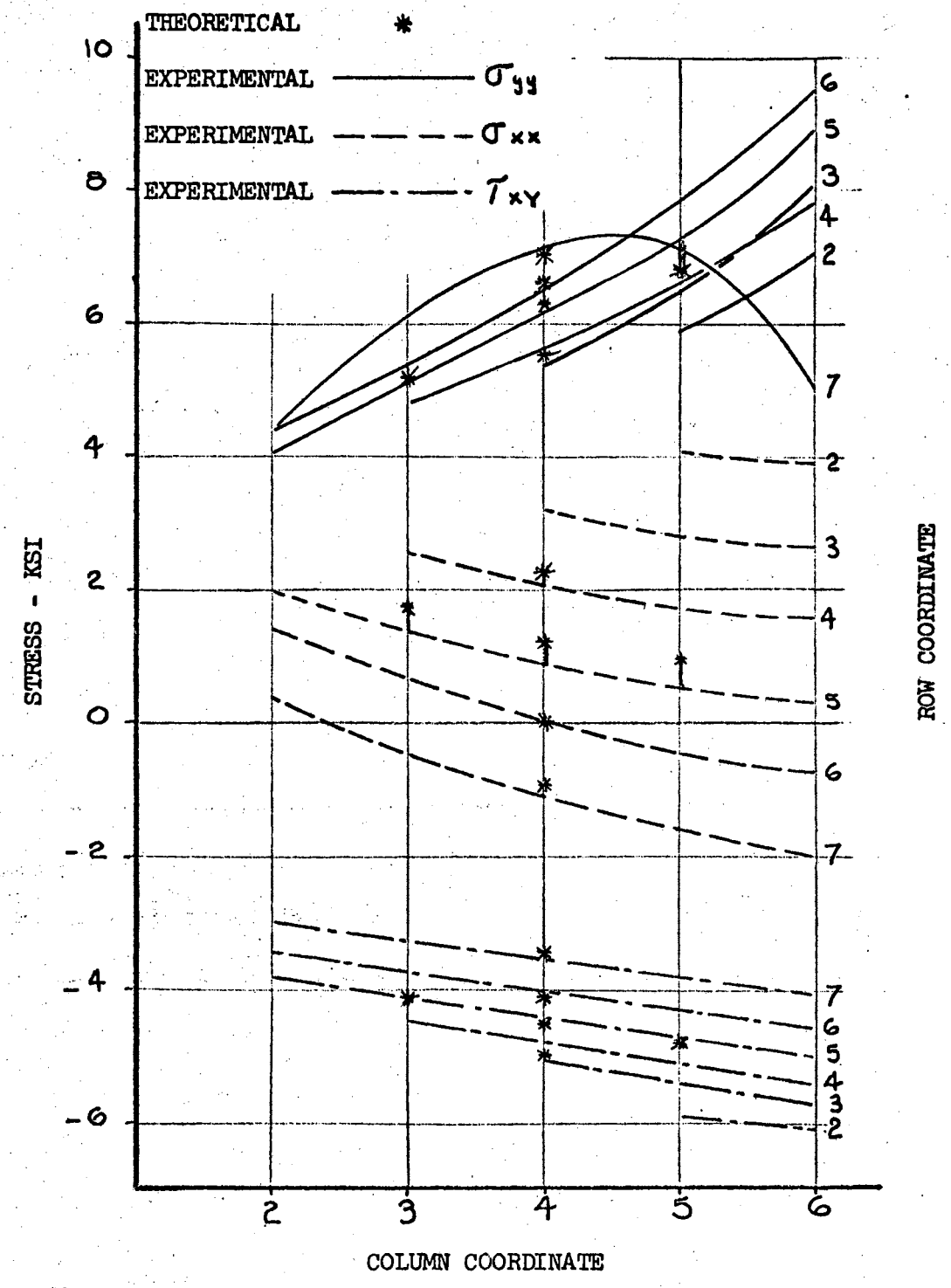

Figure 16. Stress Comparison - "Two-Mesh" Coarse

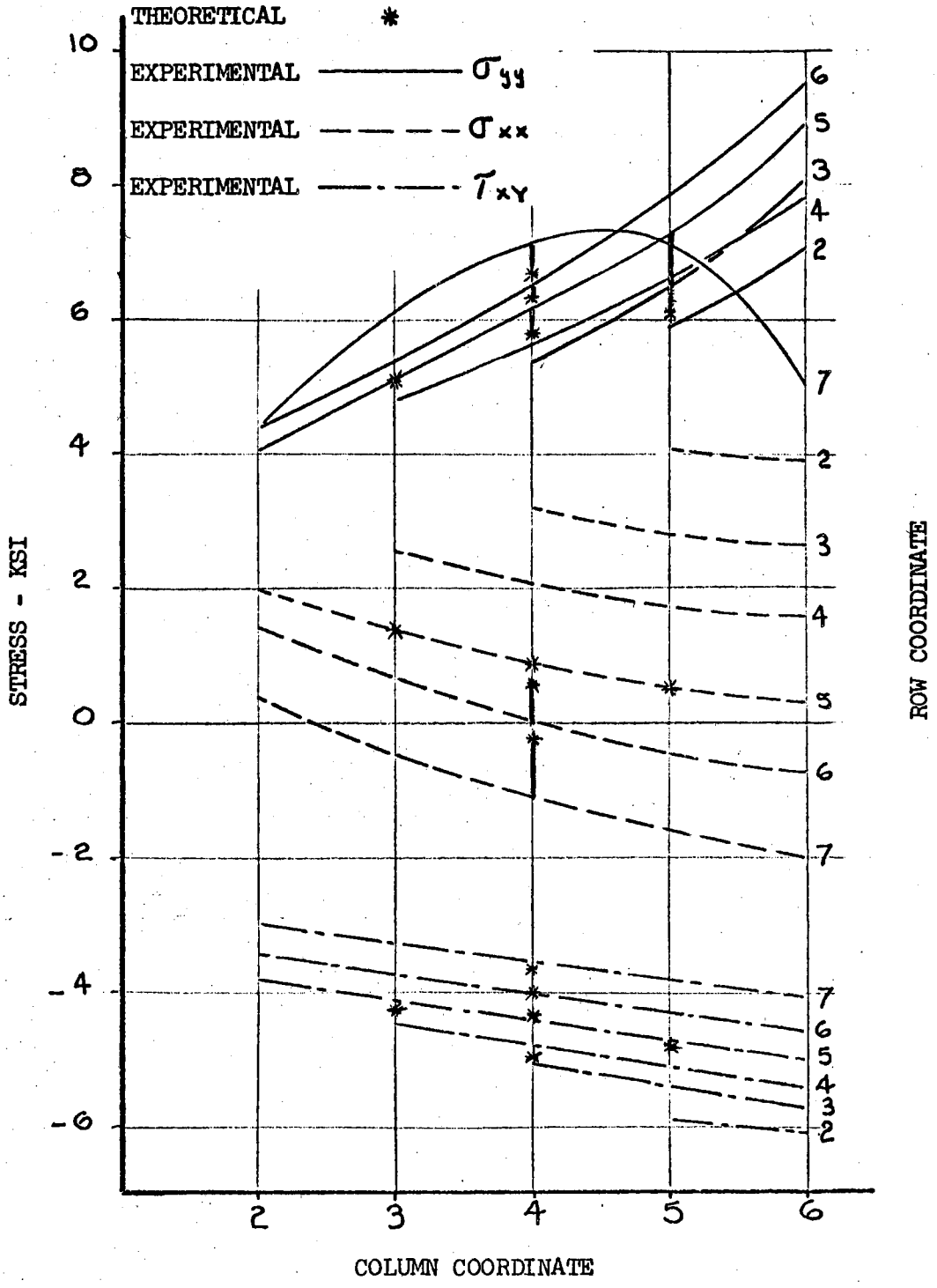

Figure 17. Stress Comparison - "One-Mesh" Coarse

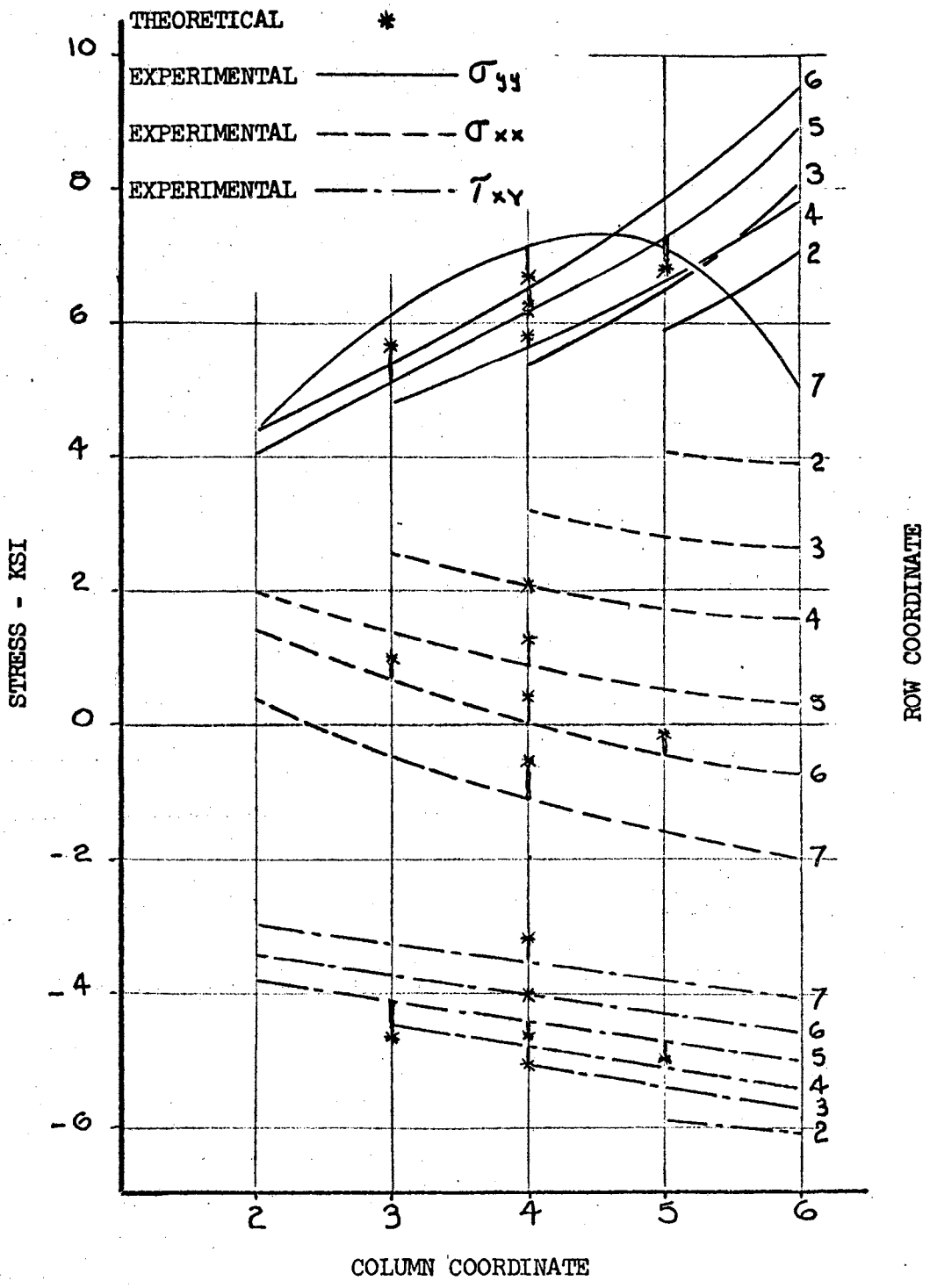

Figure 18. Stress Comparison - "Two-Mesh" Fine

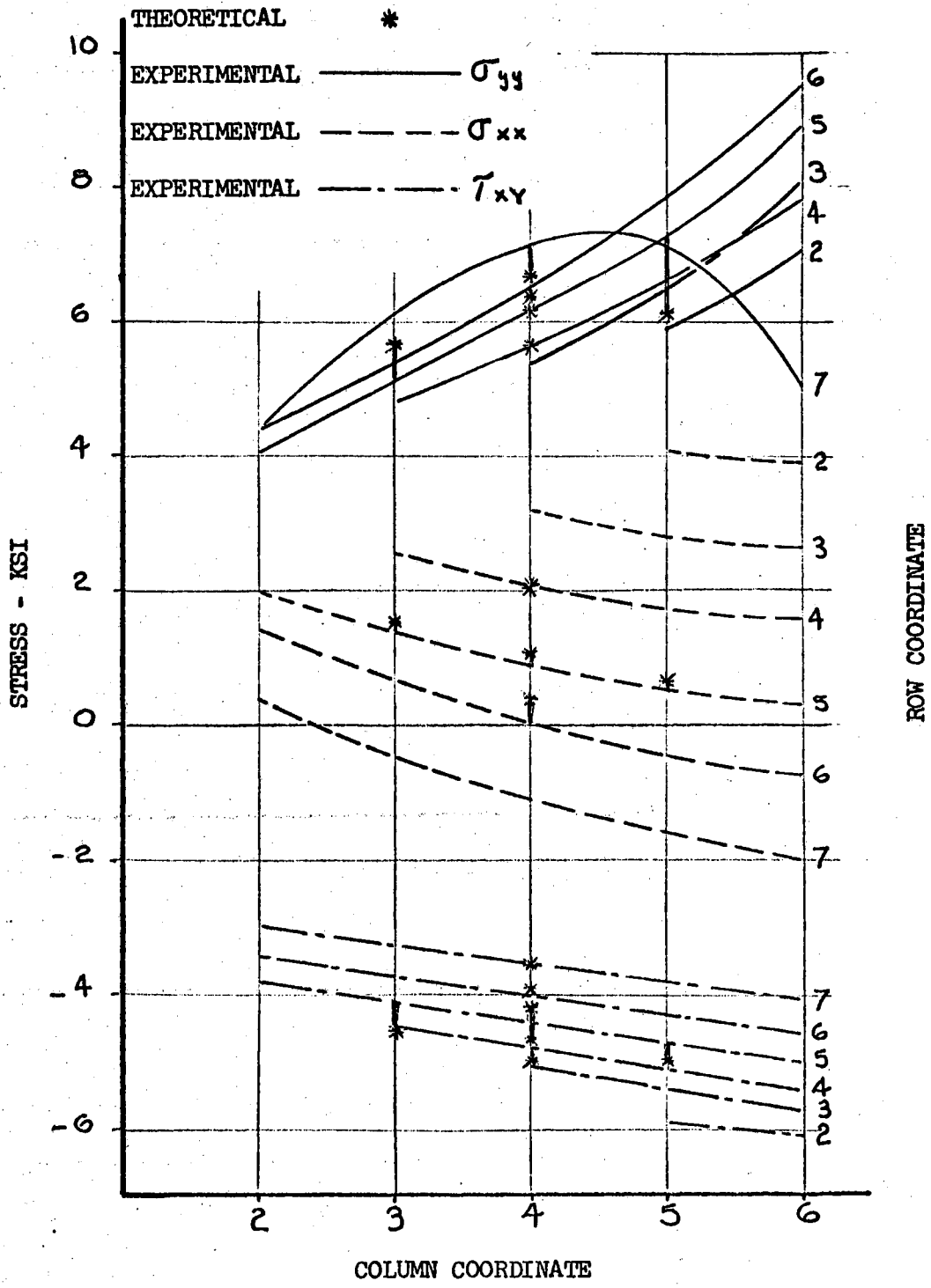

Figure 19. Stress Comparison - "One-Mesh" Fine

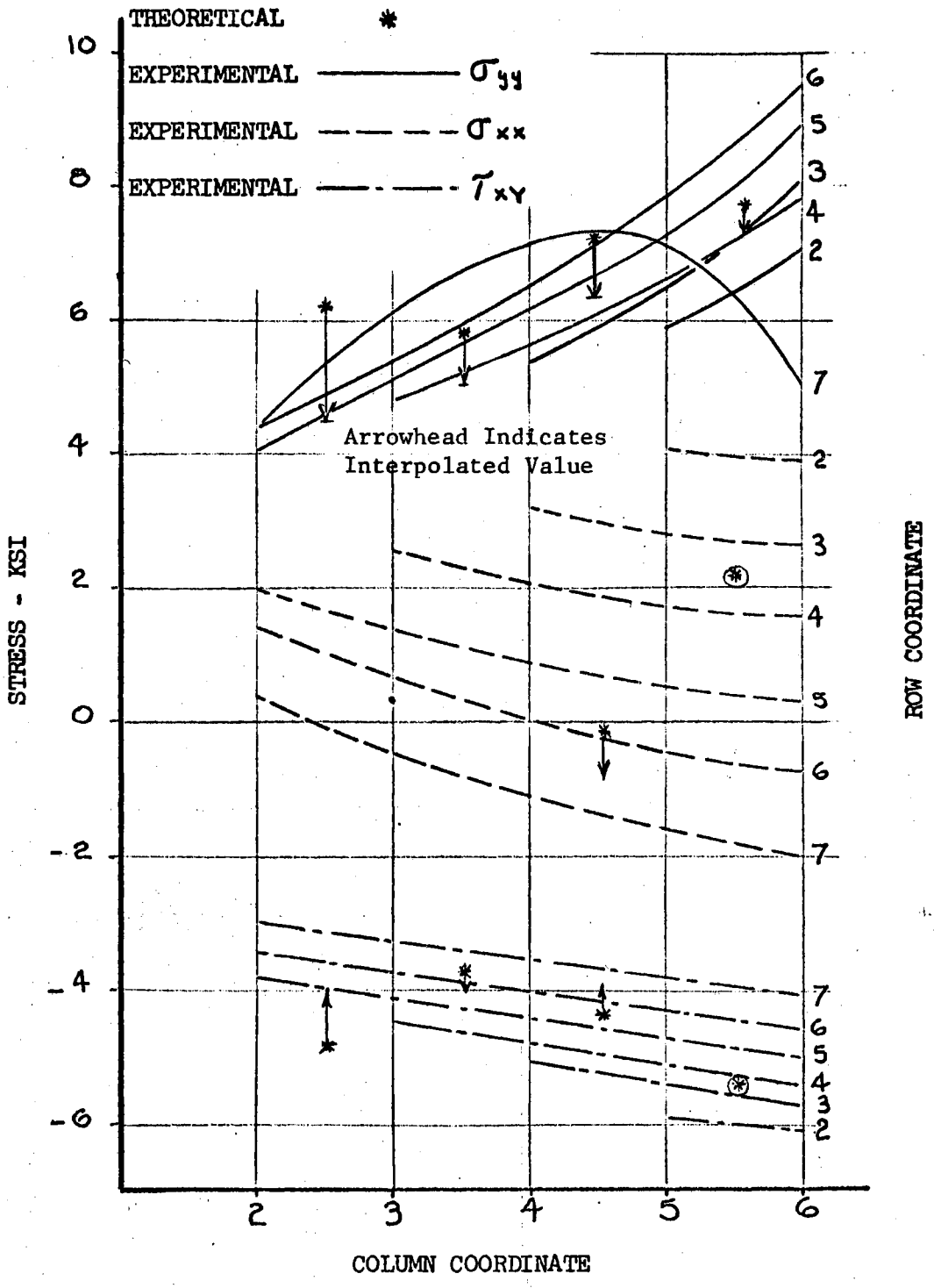

Figure 20. Stress Comparison - Direct Stiffness Method

Ancillary Experiments

Ancillary experiments were conducted during the main experiment. The more important experiments were: ultrasonic measurement of web thickness, optical measurement of deflections, photoelastic coating measurement of web strains, and aerosol Stresscoat strain measurements.

The thickness of the bulkhead web and vertical coamings were measured by use of the Vidigage, an ultrasonic thickness tester. Vidigage Model 21 is manufactured by Branson Instruments, Incorporated, Stanford, Connecticut. The paint was removed by sanding in the spots where the thickness was measured. The instrument was "readied" by measurement of a test sample of approximately the same material and thickness as the specimen. The test sample was measured with a micrometer. Ultrasonic measurement is made by the bright peak on the face of the instrument. Knob settings for the web were: "Standard", contact 2, sensitivity 2, initial setting 8.31. Measurements were estimated to be within ±.001 inch.

Deflections were measured optically with a Wild N-III sight level and Brunson Model 71 Jig Transit. Vertical and horizontal measurements from a space reference coordinate system were measured at two locations. Vertical scales were attached to the outstanding leg of the tee extrusion at top dead center. The transit was "bucked-in" on two horizontal scales. Line of sight was established parallel to the axis of the cylinder. Deflections were measured optically at zero load. "Rezeroing" with the optical mike and recording the position provided desired measurements. Deflection behavior was found to be a complicated combination of pitching up and heaving to the east. Measurements agreed within .007" at the jig end but were .030" at the bulkhead end.

Plastic sheet from Photolastic, Incorporated was bonded to the bulkhead web on the side opposite and above the strain gaged region. Satisfactory readings could not be obtained because the jig obstructed a normal view. The color plate is not included in the document because the obliquity prevented clearness of the isochromatics. The coating, type PS-2-A, .124" thick, was obtained from Photolastic, Incorporated. Visual inspection with the hand-held polariscope revealed the local stress concentration effects of the fasteners.

A new form of brittle lacquer, ST-101 Aerosol Stresscoat, was used on this experiment. The new material was donated by the Magnaflux Corporation for use on this project. ST-75X was applied to the bulkhead web and the cylinder skin while load was held on the specimen for several hours. Upon relaxing load, cracks were barely visible near the bolted flange of the vertical coaming. The new lacquer has the advantage of being insensitive to humidity (the old lacquer was very sensitive), but could not be red-etched without "erasing" the crack pattern. The classical 45^{o} crack pattern was visible in the skin under torsion. The photograph was obtained without red etchant. Light rays were directed in a plane normal to the cracks and approximately 45^{o} to the surface of the skin.

CHAPTER IV

SUMMARY AND CONCLUSIONS

Summary

Two main objectives were achieved by this research work and are reported: development of a new two-dimensional stress analysis method, and measurement of a very large set of experimental data from a uniquely designed structural specimen. The first main contribution is a versatile analysis method capable of solving the plane stress problem for irregularly shaped membranes that occur so frequently in marine and aircraft stress analysis. The new method is direct and suitable for immediate use by the practicing engineer. The resulting analysis method has the features of the classical finite difference method, the relaxation method, and the methods of matrix algebra. The heart of the anslysis method is the biharmonic boundary value integration. Digital computer programs were developed for the biharmonic line integration and for the calculation of stresses from the Airy Stress Function.

The analytical procedure suggested for the proposed method is:

1. Make a scaled drawing. Lay out grid.
2. Identify and number nodes.
3. Perform external equilibrium check.
4. Calculate boundary Φ's.
5. Tabulate numerical data.

6. Set up equations of unknowns.

7. Tabulate matrix coefficients.

8. Solve simultaneous equations.

9. Use phi output to calculate stresses.

The restrictions on the analysis method are described in this paragraph. The membrane can be described as a simply connected region with a piecewise smooth contour. Material in the membrane is homogeneous, isotropic, and obeys Hooke's law. A plane, isothermal, static stress conditions exist with resulting infinitesimal strains. Body forces are considered to be negligible.

A second main contribution consists of a large, unique body of experimental evidence for a membrane having an irregular geometric boundary loaded with a complex distribution of shears and tractions. Strain rosettes are very closely spaced and the experimental data volume produced is larger than previously available in the literature. Although the experiment was designed for a point-for-point correlation to the newly developed analysis procedure, it is suitable for comparison to alternate analytical methods.

The test specimen had a minimum of "idealizations" frequently used in past researches. Actual skins, extrusions, frames, fittings, and tapered shank fasteners were used in the same way as they are in aircraft structures. Complications such as these were purposely introduced to surround the test region with "elastic sea" necessary to achieve the desired distribution shear flows and normal loads on the boundaries. Experimental information of this kind is absent in published literature. These newly obtained experimental data were also compared to a well-established analytical method.

Ancillary experiments employing optical tools, ultrasonic measurement, photoelasticity and brittle lacquer were conducted. The highlights of these experiments are included for the interested reader.

Conclusions

The theoretical and experimental correlation was within ±300 psi for the central nodes, but varied 1300 psi in the upper right-hand corner. High experimental stresses could have been caused by local contact strain originating at the fastener holes. Since the analytical method gives stress values which are lower than those derived by experiment, caution should be used if this method is used for final analysis or web gage selection.

The direct stiffness method of analysis also agreed well with the newly obtained experimental data. The excellent correlation of analysis methods was anticipated by the preliminary theoretical work by Chapel and Smith [11].

The worth of the method was proved by the theoretical and experimental data generated in this study. Results warrant further development and continuation. Specific recommendations are noted below and a suggested course of action is offered for the benefit of future investigators. It is recommended that this method be used in applications that arise during the design, strength checking, and stress analysis of plane irregular membranes.

Recommendations

1. Other shapes and loadings should be investigated theoretically and experimentally. Extension of this work to include regions with multiply connected irregular contours should be investigated. Nets other than square should be explored when the boundary shape or loading suggests it.

2. Displacement boundary conditions and mixed boundary conditions are logical extensions of the present work.

3. For thin webs, it is recommended that strain gages be installed "back-to-back" on the structure.

4. The effects of body forces should be investigated for applications where boundary stresses are light. When web depth-to-thickness ratio is high, buckling may occur at low stresses.

5. Thermal stresses and strains were not included in this analysis. Applications involving irregular webs under thermal gradient may warrant extension of the method to include this variable.

6. Analysis suitable for irregular plate bending problems could be devised by including the non-homogeneous plate stiffness terms.

7. Several small digital computer programs were used in the analysis. These programs could be linked together to form a continuous analysis method. Other computer economies could be sought. Input requirements should be minimized for repetitive problems.

8. Other experimental structures having irregular boundaries should be investigated to broaden and strengthen the analysis method. The same specimen could be used by successive modifications such as progressive cut-out methods.

9. Other experimental media could be used to advantage. In cases involving heavy webs (possibly ship, submarine, and civil structures) photoelastic coating methods are recommended.

10. The cubic polynomials, trigonometric functions, hyperbolic function, fourth degree polynomials, and function combinations that satisfy the biharmonic equation may significantly improve the accuracy of the solution near the boundary. This study may be conducted for a variety of shapes on wholly theoretical grounds. Nonlinear stress gradients may be treated with other combinations of biharmonic functions.

11. Poisson's ratio enters the experimental stress calculations. Precise values of this particular material constant are needed for commonly used construction materials.

12. Future experiments involving large numbers of closely spaced rosettes may be greatly simplified by use of new strain gage bonding techniques such as the Rokide process of Baldwin-Lima-Hamilton [12]. It is recommended that small groups of gages be bonded before attempting a large number such as that used during the subject experiments. Each gage was installed individually during this work, consuming months of time. It may be possible to install large groups by locating all gages, then spraying all at once.

13. Strain gages near the boundary of a region are subject to error arising from high local stresses. Gages near highly loaded fasteners are especially prone to local stress concentrations. It is recommended that the local stresses be determined by a field measurement method before placement of the strain gage. If the field method is photoelastic or Moiré, a clear view of 90^{o} should be provided. If brittle lacquer ("Stresscoat") is used, it is recommended that the "Statiflux" etchant be tried, [13].

14. It is recommended that "Airy" surface and shear surface plotting be continued whenever possible. Other structural applications and other plotters may be used. It is also recommended that isobars, isoclinics, and the classic plots be explored. Maxima and minima may be found. These graphical data may then be used for possible weight savings (low stressed areas may be removed) or for recommending hole locations for wire bundles, tubing, cables, and other inevitable cutouts.

15. The analytical method developed here should be explored to devise plate elements for use in the matrix force and matrix displacement methods of analysis. It is possible that the proposed method be construed as a sub-routine in the finite element methods, or conversely, output from finite element methods could be used as input to the proposed method.

A SELECTED BIBLIOGRAPHY

1. Theodorescu, P. P., "One Hundred Years of Investigations in the Plane Problem of the Theory of Elasticity", Applied Mechanics Review, Vol. 17, No. 3 (March 1964), pp. 175-186.

2. Timoshenko, S. P. and Goodier, J. N., Theory of Elasticity, McGraw-Hill Book Company, Inc., 2nd Edition (1951).

3. Allen, D. N. de G., Relaxation Methods in Engineering and Science, McGraw-Hill Book Company, Inc., New York (1954), pp. 105-124.

4. Airy, G. B., "On the Strains in the Interior of Beams", Philosophical Transactions, Royal Society of London, Vol. 153 (1863), pp. 461-493.

5. Shaw, F. S., An Introduction to Relaxation Methods, Dover Publications (1953).

6. Boeing Document D2-4513, "COSMOS, A Computer Program for Structural Analysis", Revised October 1964.

7. Turner, M. J., et al. "Stiffness and Deflection Analysis of Complex Structures", Journal of the Aeronautical Sciences, Vol. 23, pp. 805-823, 845, 1956.

8. Boeing Drawing 35-26401, Revision B, "Test Installation - Elastostatic B.V.P.", November 1966 (4 sheets).

9. Boeing Drawing 35-21491, Revision A, "Jig Assy - Torsion Test Jig", April 1965 (7 sheets).

10. Boeing Drawing 35-26994, Revision A, "Strain Gage Installation - Elastostatic B.V.P.", January 1967.

11. Chapel, R. E. and Smith, H. W., "Finite Difference Solution for Plane Stresses", (unpublished paper submitted to AIAA Journal, June 7, 1967).

12. Product Data 200-3, "The Rokide Process and Equipment - The Universal Sensor Application", Baldwin-Lima-Hamilton Electronics, Waltham, Mass., July 1966.

13. Staats, H. N., "Principles of Stress Coat; A Manual for Use With the Brittle Coating Stress Analysis Method", Magnaflux Corp., 1955.

VITA

Howard Wesley Smith

Candidate for the Degree of

Doctor of Philosophy

Thesis: THE BIHARMONIC BOUNDARY VALUE PROBLEM AS APPLIED TO A MEMBRANE HAVING IRREGULAR SHAPE

Major Field: Mechanical Engineering

Biographical:

Personal Data: Born in New York City, November 24, 1929, the son of Albert E. and Rose M. Smith.

Education: Received the Bachelor of Science degree Cum Laude, 1951, and the Master of Science degree, 1958, from Wichita State University with a major in Aeronautical Engineering; completed the requirements for the Doctor of Philosophy degree in May 1968.

Professional Experience: Joined The Boeing Company August, 1950; Jr. Engineer 1951; Stress Analyst on B-47 bomber airplane program; Structures Engineer in research and preliminary design; Stress Research and Development Group Supervisor, 1959; Principal Investigator on Contract No. AF 33(616)-8036, Project No. 1(8-7381), Task No. 738103; Structures Research Manager, January, 1965, to date. Co-principal Investigator on Grant AF-AFOSR-1153-66.

Professional Organizations: Registered Professional Engineer, Kansas License 4591; Associate Fellow, American Institute of Aeronautics and Astronautics; Member, Society for Experimental Stress Analysis.

Honors and Awards: Elected to honorary fraternities ΣΓΤ Aeronautics; Π ΜΕ Mathematics; ΔΕ Science; Τβ Π Engineering; Boeing Doctoral Scholarship in Wichita, 1963.